Memorandum of Understanding 1907105/NL/CP

Université Blaise Pascal LGCB
Laboratoire de Génie Chimique et Biochimique

TECHNICAL NOTE: 83.2

UPGRADING THE RADIANT LIGHT TRANSFER MODELLING IN RECTANGULAR OR CYLINDRICAL PHOTOBIOREACTORS

-

THEORETICAL ASPECTS

prepared by/*préparé par*	J.-F. Cornet, J. Deremetz, C.G. Dussap
reference/*réference*	ESA/ESTEC Contract
issue/*édition*	1
revision/*révision*	0
date of issue/*date d'édition*	
status/*état*	Draft
Document type/*type de document*	Technical Note
Distribution/*distribution*	MELiSSA all

CONFIDENTIAL DOCUMENT

APPROVAL

Title *titre*	Upgrading the radiant light transfer modelling in rectangular or cylindrical photobioreactors-theoretical aspects	issue *issue*	**Error! Reference source not found.**	revision *revision*	0

author *auteur*	J.-F. Cornet, J. Deremetz, C.G. Dussap	date ## *date*

approved by *approuvé par*		date *date*

CHANGE LOG

reason for change /*raison du changement*	issue/*issue*	revision/*revision*	date/*date*

CHANGE RECORD

Issue: **ERROR! REFERENCE SOURCE NOT FOUND.** Revision: 0

reason for change/*raison du changement*	page(s)/*page(s)*	paragraph(s)/*paragraph(s)*

TABLE OF CONTENTS

INTRODUCTION

In the 90's, the LGCB developed knowledge models for photobioreactors (PBR) of the MELiSSA project with first applications to the photoautotrophic cultivation of *Arthrospira platensis* (Compartment IVa), and then to the photoheterotrophic cultivation of *Rhodospirillum rubrum* (Compartment II). They met some successfulness in term of simulation; scale-up and model based predictive control for the C IVa, and provided recently a qualitative knowledge of the very complex behaviour of the C II operating in continuous conditions (Cornet *et al.*, 2005 – TN 55.1). Nevertheless, even if they presented an intrinsic coherence, these models had limited range of validity and robustness, because they rely on the independent experimental determination of several parameters, for both the radiative transfer part and so formulating the kinetic or stoichiometric coupling. Moreover, in most applications, the radiative transfer problem was treated using a simple isotropic two-flux model which is far to be sufficiently realistic to overcome a so difficult problem as the sub-critical bifurcation appearing for example in continuous cultures of *Rs. rubrum*.

Ever after, a considerable amount of theoretical work has been performed in LGCB with the objective of increasing the robustness and the predictive character of the models by a reification of their parameters. This means that an *a priori* theoretical determination of the radiative, kinetic and stoichiometric parameters involved in the PBR modelling is sought from only very basic information for any considered micro-organism (shape, size distribution and pigment content). The different stages involved in building a so-called reified model for PBR was recently summarised and published as a general scheme defining "the royal route toward a predictive and robust knowledge model for PBR engineering purposes" (Cornet *et al.*, 2003). Roughly speaking, this approach requires to manage first the predictive radiative transfer problem inside a PBR of any given design (geometry and boundary conditions), and second the local and spatial coupling, with resulting rates and stoichiometries. Moreover, a thorough analysis of the characteristic time of each successive process involved is required to discriminate between limiting steps and their possible coupling with hydrodynamics.

The aim of the work discussed in the current MELiSSA contract consists in developing, from the recent theoretical and experimental results obtained in LGCB, a new generation of models for the radiative transfer in PBR of different geometries, in order to up-grading the models available in the MELiSSA team which are now completely obsolete as previously discussed (even if they provide correct results in term of biomass productivities because of their own intrinsic coherence). Particularly, this technical note presents the theoretical part of the reification of the radiant light transfer problem in PBR (the experimental validation being reported in the next TN 83.3). The following points are successively addressed:

- predictive calculation of the optical properties for photosynthetic micro-organisms, i.e. the real and imaginary part of their complex refractive index;
- derivation of the radiative properties for micro-organisms of different shapes (the like-cylinder shape is retained in this TN as an example fitting well with *Rs. rubrum*

and *Arthrospira platensis*) by solving the Maxwell equations of electrodynamics. These properties are the spectral mass absorption coefficient Ea_{λ}, the spectral mass scattering coefficient Es_{λ}, and the phase function for scattering $p_{\lambda}(\Omega,\Omega')$ which describes the anisotropy of the photon scattering by the particles;

- the one-dimensional resolution of the radiative transfer equation (RTE) in Cartesian and curvilinear systems of coordinates, using both an approximate generalised two-flux method, and a rigorous sophisticated numerical method.

The final results obtained with different assumptions or averaging methods for irradiances, light flux densities or local volumetric rates of radiant energy absorbed, are discussed in term of accuracy and calculation time in order to provide to all the users in the MELiSSA team, the keys in choosing the best appropriate solution corresponding to their engineering purpose (simulation, design, scale-up, control…). Even if this work is mainly discussed in the framework of the C II modelling (requiring a more refined treatment of the radiative transfer problem than for example the C IVa), we adopted a general presentation for each theoretical point reviewed, so the method is clearly applicable for *Arthrospira platensis* or any new micro-organism which could be involved in the MELiSSA project.

Finally, the authors are wedded to formulate an important notice to the readers. The work summarised in this TN represents a considerable amount of concepts, theoretical developments and calculations dealing with different fields of physics, and it appeared very difficult to write a concise, comprehensive and self-consistent text for the non-specialist reader in the form of a technical note. This work is in fact an important part of the French diploma "Habilitation à Diriger des Recherches" of one of the authors which should be published in 2007. For this reason, and to avoid very complex and lengthy developments in this TN, we have often referenced to this manuscript as (Cornet – HDR) in the text. All the details of the general approach only sketched in this TN will be available in this monograph for the inquisitive reader. Nevertheless, from a theoretical point of view, the content of this TN is likely difficult to understand since, from our knowledge of the literature, there is no other team in the world, in any field of physics, which is able to manage the problem of radiative transfer with a so high degree of sophistication (mainly, using the exact radiative properties in solving rigorously the RTE). It should only be kept in mind that several practical numerical codes (Fortran or Matlab®) have been developed, tested and validated in LGCB. Even if they have an intrinsic complexity, they can be used easily (except the problem of calculation time for radiative properties) inside the MELiSSA team with applications regarding *Arthrospira platensis*, *Rhodospirillum rubrum*, or any new micro-organism of interest in the future. The resulting knowledge models are then more robust and predictive and the new inner complexity is not a problem for users because the complete structure of the model remains roughly the same and all the one-dimensional assumptions can still be used, from the more simple two-flux approximation to a rigorous high order numerical method. They are all easily tractable as soon as a "plug and play" solution was provided by LGCB.

1 RADIATIVE PROPERTIES OF PHOTOSYNTHETIC MICRO-ORGANISMS

Photobioreactors are characterised by complex particulate and participative material phase interacting with a photonic phase by absorption and scattering phenomena, both related by the radiative transfer theory and modelling. The radiative properties of the culture broth, i.e. the so-called absorption and scattering cross sections with the phase function for scattering are prerequisite data of prior importance because they appear as parameters in the radiative transfer equation, enabling the calculation of the (highly-heterogeneous) radiation field inside the reactor. In case of submerged cultures of photosynthetic micro-organisms, neglecting the optical properties of the culture medium itself and assuming an elastic scattering process, these radiative properties are those of one micro-organism, the determination of which is far to be a trivial problem, mainly because these kinds of particles present a conducting behaviour, an intrinsic heterogeneity and a great variety of shapes. The two former points are related to the optical properties of the micro-organisms which must be necessarily calculated by a predictive mean before any assessment of the radiative properties themselves (Pottier *et al.*, 2005).

Actually, the radiative properties of micro-organisms depend first of their pseudo-homogeneous optical properties, i.e. the complex refractive index m_λ (which is a spectral quantity), their shape and their size parameter x (a ratio between a characteristic size and the considered wavelength λ). The theoretical link between these data and the radiative properties of the medium is established by calculating the far electric and magnetic fields, the vector product of which giving the Poynting vector field, i.e. characterising the radiant light energy absorbed and scattered by the particle. This requires solving the Maxwell equations for electromagnetism in spherical coordinates, considering the particle as a linear, isotropic and homogeneous medium (regarding optics), then gives rise to the well known (for spherical shape at least) Lorenz-Mie theory (Van de Hulst, 1981; Bohren and Huffman, 1983). The radiative properties are then deduced from the spatial distribution of amplitudes and phases of incident and scattered waves, considering natural unpolarised light in our case (see hereafter).

1.1 *Optical Properties of Photosynthetic Micro-organisms*

1.1.1 HOMOGENEOUS PARTICLE

Any homogeneous material is optically characterised by its refractive index m_λ. If the material is only a dielectric (an insulator), this refractive index is real, but if the material is a conductor, as it is the case for photosynthetic micro-organisms which are weak conductors in the visible spectrum, the refractive index is complex. If the particle is suspended in any other material (different of the free space and with a refractive index n_m) it is more convenient to work with the relative refractive index $m_{r,\lambda}$, defined from (with a convention retaining only the $e^{i\omega t}$ terms):

$$\boxed{m_{r,\lambda} = \frac{m_\lambda}{m_{m,\lambda}} = \frac{n_\lambda}{n_m} - i\frac{\kappa_\lambda}{n_m} = n_{r,\lambda} - i\kappa_{r,\lambda}} \quad (1)$$

where n_m is the (real) refractive index of the medium surrounding the particle, n_λ and κ_λ, respectively the real and imaginary part of the refractive index for the particle. These physical properties are related (Bohren and Huffman, 1983) to the well-known real (ε_r') and imaginary (ε_r'') dielectric constants by the following equations of change (omitting the λ indices for convenience):

$$\varepsilon_r^{'} = n^2 - \kappa^2 \quad (2)$$

$$\varepsilon_r^{''} = 2n\kappa \quad (3)$$

$$n = \sqrt{\frac{\sqrt{\varepsilon_r^{'2} + \varepsilon_r^{''2}} + \varepsilon_r^{'}}{2}} \quad (4)$$

$$\kappa = \sqrt{\frac{\sqrt{\varepsilon_r^{'2} + \varepsilon_r^{''2}} - \varepsilon_r^{'}}{2}} \quad (5)$$

Moreover, the imaginary part of the refractive index κ_λ, defining the ability of a given medium to absorb the radiation, is directly linked to the absorption coefficient for the cell material (which is not the absorption coefficient of the particle!) by the relation (Bohren and Huffman, 1983):

$$\boxed{a_{cm,\lambda} = \frac{4\pi\,\kappa_\lambda}{\lambda_0}} \quad (6)$$

Equations (1 to 6) define the so-called optical properties for any pseudo-homogeneous particle submerged in a liquid medium (for our purposes), and need to be determined by a predictive mean involving each of the cellular dielectric (membrane, cytoplasm…) or conducting (pigments) components. The imaginary part κ_λ, responsible for absorption, is indeed strongly related to the wavelength, depending of the pigment content of a given micro-organism, and its calculation on the active spectrum for photosynthesis, which is not a trivial problem, will be presented in the next paragraph. At the opposite, the relative real part $n_{r,\lambda}$ of the refractive index may be shown as a weak function of wavelength in the visible spectrum, and it can be considered as a constant with a very good approximation. It is then possible to determine the particular value of n_r for a given micro-organism from the knowledge of the volume fraction of its main components (Wyatt, 1968 and 1972), using general composition rules (see hereafter), or by experimental inverse method (Cornet - HDR) at any non-absorbed wavelength. In a first approach, the optical properties of the micro-organism alone (i.e. without any intracellular substance of reserve) must be found, then indeed, if the considered strain may accumulates some polymers (as polyhydroxybutyrate PHB for *Rs. rubrum*), a general relationship is needed to take into account the corresponding variations in the real part of the refractive index.

1.1.2 PREDICTIVE CALCULATION OF THE *IN VIVO* SPECTRAL IMAGINARY PART FROM PIGMENT CONTENT

The predictive calculation of the spectral imaginary part of the refractive index κ_λ, responsible for absorption of light, is theoretically possible from the knowledge of two basic informations. First, it is necessary to know with some accuracy the mass pigment content ($w_{pig.i}$ for species i) of the given micro-organism. It is really a simple point when the pigment content does not change significantly with the culture conditions (as for *Arthrospira*), but it is not so trivial when this content is strongly influenced by the degree of light limitation in the PBR (as for *Rs. rubrum*). Second, because this optical property is strongly wavelength-dependent, one needs a data bank giving the *in vivo* mass absorption coefficient spectrum for each kind of pigment involved. This is a rather complicated problem of documentation, because most of the absorption pigment spectra in the literature are obtained in organic solvents, leading to a more or less (10 to 100 nm) important shift in the wavelength location for the absorption maxima and minima, in comparison with the *in vivo* conditions. A small data bank is available for the more representative pigments of classical photosynthetic micro-organisms (Bidigare *et al*., 1990) as phytoplankton and microalgae. Unfortunately, for purple bacteria, this kind of information is not available and we have enriched and developed the data bank with our own experimental determinations (e.g. the Bacteriochlorophyll *a* for *Rs. rubrum*).
From these preliminary data, i.e. the wavelength dependent (to every one or two nanometres if possible) mass absorption spectrum $Ea_{pig.i}$ (λ) for each kind of pigment i, it is then possible to write the intracellular cell material absorption coefficient combining eq. (6) and the convolution of all pigment spectra:

$$a_{cm,\lambda} = \frac{4\pi\,\kappa_\lambda}{\lambda_0} = \sum_{i=1}^{N} Ea_{pig.i}(\lambda).C_{pig.i} \qquad (7)$$

Then, introducing the density of the dry mass ρ_{dry}, the volume fraction of water x_w in the considered micro-organism and the pigment content w_{pig} (kg pigment / kg dry mass), gives the final relation for the *in vivo* spectral imaginary part of the refractive index on the photosynthetically active radiation domain (i.e. [400 – 900 nm] for *Rs. rubrum*):

$$\boxed{\kappa_\lambda = \frac{\lambda_0}{4\pi}\rho_{dry}\frac{1-x_w}{x_w}\sum_{i=1}^{N} Ea_{pig.i}(\lambda).w_{pig.i}} \qquad (8)$$

This relation, recently published (Pottier *et al*., 2005), is of crucial importance in modelling the optical properties of photosynthetic micro-organisms and may be applied to the particular case of *Rs. rubrum* with only two kind of pigments, the total carotenoïds and the bacteriochlorophyll *a*.

1.1.3 CALCULATION OF THE MEAN (WAVELENGTH AVERAGED) VALUE OF THE IMAGINARY PART OF THE REFRACTIVE INDEX

Clearly, the previous approach, giving the wavelength independent real part and the spectral imaginary part of the refractive index for any micro-organism is self-consistent and enables the calculation of the spectral radiative properties of the particle (see hereafter paragraph 1.4 and 1.5). Nevertheless, it is often convenient to work with mean radiative properties in wavelength (as it is currently the case for photobioreactor modelling in the MELiSSA team) in order to avoid tedious spectral calculations in solving the RTE. Acceding the mean radiative properties is of course always feasible *a posteriori* by averaging the spectral properties, but this requires 300 (or 500 for *Rs. rubrum*) calculations which may become very CPU time consuming (depending of the size parameter). For this reason, if the assumption is accepted (with regard to the accuracy of the final result), it is of prime interest to develop a method giving directly the wavelength averaged imaginary part of the refractive index κ in order to obtain the mean radiative properties in only one operation.

Evidently, the first stage consists in averaging the spectral optical properties κ_λ over a considered range of wavelength $\Delta\lambda$ (between the minimum λ_m and maximum λ_M wavelengths) but it gives only a first estimate $\kappa^\bullet$ of the best suitable value because the Lorenz-Mie theory postulates a non-linear behaviour of the radiative properties with the wavelength:

$$\kappa^\bullet = \frac{\int_{\lambda_m}^{\lambda_M} \kappa_\lambda \, d\lambda}{\Delta\lambda} \qquad (9)$$

Taking into account this non-linearity and making a substitution of the wavelength λ variable by the $\zeta = 4x\kappa_{r,\lambda}$ parameter (in which the mean size parameter $x = 2\pi\, a\, n_m / \lambda$ where a is the mean radius or the mean characteristic semi-axe for the particle), it can be shown (Cornet - HDR) that a correction factor $Q^\bullet$ must be calculated as follows:

$$\boxed{Q^\bullet = \frac{3}{2\,\Delta\zeta\, Q^\bullet(\zeta^\bullet)} \left[\begin{array}{c} \ln\left(\dfrac{\zeta_M}{\zeta_m}\right) + \dfrac{1}{\zeta_M^2} - \dfrac{1}{\zeta_m^2} + \dfrac{1}{\zeta_m\, \mathrm{e}^{\zeta_m}}\left(1 + \dfrac{1}{\zeta_m}\right) - \dfrac{1}{\zeta_M\, \mathrm{e}^{\zeta_M}}\left(1 + \dfrac{1}{\zeta_M}\right) \\ + \,\mathrm{Ei}\,(1, \zeta_M) - \mathrm{Ei}\,(1, \zeta_m) \end{array} \right]} \qquad (10)$$

In this equation, we have used successively $\zeta^\bullet = 4x\kappa_r^\bullet$, $Q^\bullet(x) = \dfrac{3}{2x}\left[1 + \dfrac{2\,\mathrm{e}^{-x}}{x} + 2\left(\dfrac{\mathrm{e}^{-x} - 1}{x^2}\right)\right]$,

and defined the so-called exponential integral as $\mathrm{Ei}\,(n, x) = \displaystyle\int_1^\infty \frac{\mathrm{e}^{-xt}}{t^n}\, dt$.

Finally, the best estimate of the mean wavelength averaged imaginary part of the refractive index for the particle is given by:

$$\boxed{\kappa = \kappa^{\bullet} Q^{\bullet}} \quad (11)$$

which may be used as a first approximation in the calculation of the direct mean radiative properties (absorption and scattering coefficients, phase function) prior to solve the RTE.

1.1.4 DIELECTRIC PROPERTIES OF HETEROGENEOUS PARTICLE – EFFECT OF THE PHB CONTENT

All the preceding developments hold in considering the micro-organism as a pseudo-homogeneous particle but it could be interesting to take into account a possible intracellular polymer accumulation by metabolic deviation, e.g. the variation in PHB content for *Rs. rubrum*. Generally speaking, the theoretical electromagnetic treatment of heterogeneous particle appears extremely difficult and up to now, only few geometrical problems have been solved by the physicist community. Nevertheless, if the considered compound presents a dielectric behaviour, some tedious theoretical considerations (Bohren and Huffman, 1983) provide useful relations of composition giving the mean optical properties of the particle from the knowledge of the particular properties of each compound themselves. In the case of PHB accumulation in the cells, the inclusions are quasi-spherical granules and probably the most powerful relation enabling the calculation of the mean real part of the refractive index for the cells is the Maxwell-Garnett equation (Bohren and Huffman, 1983):

$$\bar{\varepsilon}_r = \varepsilon_{r,m}\left[1+\frac{3 f_{PHB}\left(\dfrac{\varepsilon_r - \varepsilon_{r,m}}{\varepsilon_r + 2\varepsilon_{r,m}}\right)}{1 - f_{PHB}\left(\dfrac{\varepsilon_r - \varepsilon_{r,m}}{\varepsilon_r + 2\varepsilon_{r,m}}\right)}\right] \quad (12)$$

In this relation, available in term of dielectric constants ε_r (see the equations of change 2 to 5), we have introduced the dielectric constant for the micro-organism $\varepsilon_{r,m}$ and the dielectric constant for the PHB ε_r respectively, with the volume fraction of the PHB f_{PHB} in the cell (depending of the culture conditions). Thus, if the PHB content and the dielectric constants are known, eq. (12) enables the predictive calculation of the real part n_r of the refractive index for *Rs. rubrum*.

1.2 Theoretical Background for Radiative Properties Calculation

The interaction between a radiation beam and a particle is a complicated problem of the electromagnetic theory, and it is not possible to treat this point extensively in this technical note. We are just interested to give some theoretical background, then introducing the important variables involved in the calculation of the radiative properties of photosynthetic micro-organisms. Roughly speaking, as explained in introduction, this calculation requires solving the Maxwell equations of electrodynamics in order to obtain the value of the far electromagnetic fields around the particle in spherical coordinates. Basically, this implies to find a general relation between the incident and scattered fields, the former being characterised by two different modes, the transverse electric (TE) or the transverse magnetic (TM) mode. Because for each mode, simple relations exist between the magnetic $\mathbf{H}$ and the electric $\mathbf{E}$ fields, it is currently admitted to work with this latter, and it can be shown (Bohren and Huffman, 1983) that the sought relation is in the form:

$$\boxed{\begin{bmatrix} E_{//sca} \\ E_{\perp sca} \end{bmatrix} = \frac{\exp\left[ik(z-r)\right]}{ikr} \begin{bmatrix} S_2 & S_3 \\ S_4 & S_1 \end{bmatrix} \begin{bmatrix} E_{//inc} \\ E_{\perp inc} \end{bmatrix}} \quad (13)$$

in which *k* is the wave number. Thus, eq. (13) defines the very important amplitude scattering matrix **S,** relating the incident and scattered fields on the particle, and involved in any electromagnetic calculation. All the elements of this matrix are function of the scattering polar angle Θ and of the azimuthal angle Φ, defining respectively a particular plane of scattering in the total solid angle Ω. Nevertheless, if we reduce our field of investigation to natural unpolarised light and rotationally axi-symetric particles (which is the case for most of the micro-organisms), important simplifications appear (Bohren and Huffman, 1983) because first, the components S_3 and S_4 vanishes, and second, the two remaining components S_1 and S_2 become independent of the azimuth Φ. Finally, with this assumption, we can conclude that all the radiative properties of particles must be deduced from the knowledge of the two complex components $S_1(\Theta)$ and $S_2(\Theta)$ of the matrix **S**, defining the amplitude and the phase for the scattered scalar wave.

Introducing now the Poynting vector $\mathbf{P} = \mathbf{E} \times \mathbf{H}$ characterising the electromagnetic energy transported by the wave, it is possible to derive the general expression of the so-called cross sections for extinction and scattering by energy balance. The detailed calculations by which the fields are linked to the previous amplitude functions are extremely complicated and can be found in the reference textbook of Bohren and Huffman (1983); we just give in this technical note the resulting final expressions defining the radiative properties of particles. In case of non-polarised incident radiation (our practical assumption), the extinction cross section (taking into account both scattering and absorption phenomena for conducting particles) C_{EXT} is then given by:

$$\boxed{C_{EXT} = \frac{2\pi}{k^2}\left[\mathrm{Re}\left\{S_1(\Theta=0)\right\} + \mathrm{Re}\left\{S_2(\Theta=0)\right\}\right]} \quad (14)$$

and the energy balance imposes:

$$C_{EXT} = C_{SCA} + C_{ABS} \quad (15)$$

Clearly, the absorption cross section C_{ABS} can be obtained if the scattered cross section C_{SCA} is preliminary calculated. This scattered cross section is linked to the phase function for scattering $p(\Theta)$ by the following relations:

$$\boxed{F(\Theta) = \frac{1}{2}\left(\left|S_1(\Theta)\right|^2 + \left|S_2(\Theta)\right|^2\right)} \quad (16)$$

$$\boxed{C_{SCA} = \frac{2\pi}{k^2}\int_0^{\pi} F(\Theta) \sin\Theta \, d\Theta} \quad (17)$$

$$\boxed{p(\Theta) = \frac{F(\Theta)}{k^2 C_{SCA}}} \quad (18)$$

It clearly appears from these relations that the phase function is normalised such as:

$$\iint_{4\pi} p(\Theta, \Phi) \, d\Omega = 1 \quad (19)$$

Even if the actual radiative properties are defined from the previous cross sections (see hereafter), it is often convenient to define the efficiencies, which are dimensionless quantities. They are easily derived from the cross sections, dividing by the particle cross-sectional area projected onto a plane perpendicular to the incident beam G_a:

$$\boxed{Q_{EXT} = \frac{C_{EXT}}{G_a}, \qquad Q_{SCA} = \frac{C_{SCA}}{G_a}, \qquad Q_{ABS} = \frac{C_{ABS}}{G_a}} \quad (20)$$

Finally, it must be pointed out that all the preceding calculations can be directly handled only if the particle is a sphere, considering one typical case of incidence. At the opposite, for any other shape of randomly oriented particle, it is necessary to average each particular value of the properties over a solid angle Ω (all the incident radiations), or in case of rotationally axi-symetric particles, over all the polar angles of incoming rays θ:

$$\boxed{\left(\overline{C}, \overline{Q}, \overline{p}\right) = \frac{1}{2}\int_0^{\pi} \left(C(\theta), Q(\theta), p(\theta)\right) \sin\theta \, d\theta} \quad (21)$$

in which θ is the angle defined from the rotationally symmetry axis in a frame associated with the particle.

1.3 Radiative Properties for Actual Photobioreactor Media

As explained in introduction and discussed elsewhere (Cornet – HDR), for photobioreactor applications, the assumption of independent scattering holds true and consequently the radiative properties of the medium (a cloud of particles without interactions between them) are directly given by the algebraic summation of the considered property of each particle. This corresponds to the following rule for cross sections:

$$\left(\overline{C}_{EXT}, \overline{C}_{SCA}, \overline{C}_{ABS}\right) = \sum_{i=1}^{N} \left(\overline{C}_{i,EXT}, \overline{C}_{i,SCA}, \overline{C}_{i,ABS}\right) \quad (22)$$

where N is the total number of particles.

1.3.1 MONODISPERSE PARTICLES

If all the particles are the same (in shape, size and optical properties), i.e. for monodisperse particles, eq (22) simplifies and then, the volumetric extinction, scattering and absorption coefficients are given from the particle number density N_p by:

$$\boxed{(e, s, a) = N_p \left(\overline{C}_{EXT}, \overline{C}_{SCA}, \overline{C}_{ABS}\right)} \quad (23)$$

It must be kept in mind that, even if the indices λ have been omitted for convenience, all these radiative properties are spectral quantities of prime interest, appearing in the RTE (see the next part of this TN).

At the opposite of eq. (23), it is clear that, considering its normalisation (eq. 17-19), the phase function for scattering $\overline{p}(\Theta)$ is independent of the particles number. Consequently, in case of monodisperse particles, the phase function of the medium as a whole is just the same as the phase function of one particle.

1.3.2 POLYDISPERSE PARTICLES

In most of the practical situations, the particles have the same optical properties and global shape, but they have not the same size. The theoretical treatment of such polydisperse suspensions requires then to know the size distribution for the considered micro-organism, i.e. for a characteristic dimension r, a function $n(r)$ normalised as:

$$\int_0^\infty n(r)\, dr = 1 \quad (24)$$

The radiative properties are then available by averaging over the size distribution from integrals in the form:

$$\left(\overline{C},\,\overline{Q},\,\overline{p}\right)=\int_{0}^{\infty}\left[\overline{C}(r),\,\overline{Q}(r),\,\overline{p}(r)\right]n(r)\,dr\equiv\int_{r_1}^{r_2}\left[\overline{C}(r),\,\overline{Q}(r),\,\overline{p}(r)\right]n(r)\,dr \qquad (25)$$

Special attention must be paid on the fact that, if these integrations are not mathematically difficult (once the experimental size distribution is characterised!), they can lead to high computing calculation time, specially for the phase function assessment which is already an angular function, sometimes difficult to compute, mainly for high size parameters x. In this case, a good approximation consists in using a monodisperse computation with a mean effective characteristic radius r_{eff} defined as follows (Van de Hulst, 1981) and named Sauter radius in chemical engineering field:

$$r_{eff}=\frac{\int_{r_1}^{r_2} r\pi r^2 n(r)\,dr}{\int_{r_1}^{r_2}\pi r^2 n(r)\,dr}\cong\frac{1}{2}\frac{\sum_{i=1}^{N} d_p^3}{\sum_{i=1}^{N} d_p^2}=r_{32}=r_{Sauter} \qquad (26)$$

1.3.3 GENERAL PRACTICAL RELATIONS FOR PARTICULATE MEDIA

Although eq. (23) completely defines the volumetric coefficients (mainly for absorption and scattering) directly involved in the RTE computation, these are not the more suitable variables for photobioreactors applications, because they depend on the particle number density (or on the biomass concentration) which may varies in time (or space) inside the reactor. For this reason, it is more convenient to introduce independent quantities such as the mass absorption and scattering coefficients respective to the biomass concentration C_X in the reactor from:

$$\boxed{\left(Ea_{\lambda},\,Es_{\lambda}\right)=\frac{(a,\,s)_{\lambda}}{C_X}} \qquad (27)$$

Clearly, using eq. (23), it is possible to calculate these coefficients directly from the cross sections provided by the electromagnetic theory and the particle number density, using the volume fraction of the particles f_v, their density ρ_p or their mean volume $\overline{V}_p$ by:

$$\boxed{\left(Ea_{\lambda},\,Es_{\lambda}\right)=\frac{\left(\overline{C}_{ABS},\,\overline{C}_{SCA}\right)_{,\lambda}\,N_p}{f_v\rho_p}=\frac{\left(\overline{C}_{ABS},\,\overline{C}_{SCA}\right)_{,\lambda}\,f_v}{\overline{V}_p C_X}} \qquad (28)$$

Finally, in many radiative transfer calculations, the assumption is made to work only with wavelength averaged coefficients in order to solve the RTE one time instead of 300 to 500 spectral computations. We have already discussed (part 1.1.3) a way in averaging first the optical properties to obtain directly the mean cross sections, but it is only an approximate method which is interesting in case of high individual computation times (polydisperse particles with high size distribution). Rigorously speaking, the mean radiative properties should be obtained by averaging the exact spectral coefficients over the considered spectrum $\Delta\lambda$ leading to perform the simple integrals:

$$(a, s, Ea, Es) = \frac{1}{\Delta\lambda}\int_{\lambda_1}^{\lambda_2}(a_\lambda, s_\lambda, Ea_\lambda, Es_\lambda)\, d\lambda \quad (29)$$

At the opposite, because the computation of a sufficiently high number of angular values for the phase function is often more tedious, it is customary to keep the previous approach in this case and to perform only one computation at the mean wavelength $\bar{\lambda}$ (depending of the emission spectrum for the radiation) from the determination of mean optical properties with eq. (11), so using:

$$p(\Theta) = p_{\bar{\lambda}}(\Theta) \quad (30)$$

1.4 Exact Calculation of Radiative Properties using the Lorenz-Mie Theory for Spheres

Until now, we reviewed the general methodology giving first the calculation of optical properties of photosynthetic micro-organisms, and then the general relations leading to the calculation of their radiative properties from the two components S_1 and S_2 of the amplitude scattering matrix, but we have not discussed the calculation itself of these components for a given shape of particle. This is the last problem that we are faced, and it is not the least because this calculation requires finally to solve the four Maxwell equations of electromagnetism around the particle in spherical coordinates. This is an extremely complicated problem leading to the famous Lorenz-Mie theory, which is still a significant field of investigation for physicists, considering non-spherical particles (if the analytical problem was solved one century ago by Lorenz and Mie for spheres, the general solution for randomly oriented spheroids was only established in 1980 by Asano).
Although few micro-organisms only have a spherical shape, it is important to develop the solutions for spherical particles because it is customary in the relevant literature to calculate the radiative properties of particles using the assumption of equivalent spheres. This last point is in fact a critical point that we will discuss in the next technical note, because it leads to very important deviations in comparison with experimental measurements. Nevertheless, it is out of the scope of this technical note to develop extensively the theory for the Lorenz-Mie problem, corresponding to complete chapters in reference textbooks (Van de Hulst, 1981; Bohren and Huffman, 1983). We just briefly summarise here the main relations involved in the radiative

properties calculation of mono- or polydisperse spherical particles. In this case, and according to our previous notations and conventions, the two components of the scattering amplitude matrix are given by:

$$\boxed{\begin{aligned} S_1(\Theta) &= \sum_{n=1}^{\infty} \frac{2n+1}{n(n+1)} \left\{ a_n \pi_n(\cos\Theta) + b_n \tau_n(\cos\Theta) \right\} \\ S_2(\Theta) &= \sum_{n=1}^{\infty} \frac{2n+1}{n(n+1)} \left\{ b_n \pi_n(\cos\Theta) + a_n \tau_n(\cos\Theta) \right\} \end{aligned}} \quad (31)$$

leading, from the definitions of radiative properties (eq. 14-18) to the final relationships for cross sections:

$$C_{EXT} = \frac{2\pi}{k^2} \sum_{n=1}^{\infty} (2n+1) \operatorname{Re}\{a_n + b_n\} \quad (32)$$

$$Q_{EXT} = \frac{2}{x^2} \sum_{n=1}^{\infty} (2n+1) \operatorname{Re}\{a_n + b_n\} \quad (33)$$

$$C_{SCA} = \frac{2\pi}{k^2} \sum_{n=1}^{\infty} (2n+1) \left(|a_n|^2 + |b_n|^2 \right) \quad (34)$$

$$Q_{SCA} = \frac{2}{x^2} \sum_{n=1}^{\infty} (2n+1) \left(|a_n|^2 + |b_n|^2 \right) \quad (35)$$

and to:

$$p(\Theta) = \frac{\displaystyle\sum_{n=1}^{\infty} \sum_{m=n}^{\infty} \frac{2n+1}{n(n+1)} \frac{2m+1}{m(m+1)} \left[\left(a_n a_m^* + b_n b_m^* \right) \left(\tau_n \tau_m + \pi_n \pi_m \right) + \left(a_n b_m^* + a_m^* b_n \right) \left(\tau_n \pi_m + \pi_n \tau_m \right) \right]}{2\pi x^2 Q_{SCA}} \quad (36)$$

for the phase function.

In these equations, we have introduced the so-called expansion coefficients a_n and b_n (a_n^* and b_n^* being their complex conjugate) from:

$$\boxed{\begin{aligned} a_n &= \frac{\psi_n'(y)\,\psi_n(x) - m_r \psi_n(y)\,\psi_n'(x)}{\psi_n'(y)\,\zeta_n(x) - m_r \psi_n(y)\,\zeta_n'(x)} \\ b_n &= \frac{m_r \psi_n'(y)\,\psi_n(x) - \psi_n(y)\,\psi_n'(x)}{m_r \psi_n'(y)\,\zeta_n(x) - \psi_n(y)\,\zeta_n'(x)} \end{aligned}} \quad (37)$$

in which the Riccati-Bessel functions $\psi_n(z)$ and $\zeta_n(z)$ are defined by $\psi_n(z) = z\, j_n(z)$ and $\zeta_n(z) = z\, h_n^{(2)}(z)$, $\psi_n'(z)$ et $\zeta_n'(z)$ being their derivative functions, all calculated from the spherical Bessel function of first kind j_n and second kind y_n, and from the second kind Hankel function $h_n^{(2)}(z) = j_n(z) - i\,y_n(z)$. Moreover, we have also used the derivative functions of the Legendre polynomials:

$$\pi_n(\cos\theta) = \frac{dP_n(\cos\theta)}{d\cos\theta}$$

$$\tau_n(\cos\theta) = \frac{dP_n^1(\cos\theta)}{d\theta}$$

Clearly, the computation of eq. (32-37) requires developing sophisticated numerical codes, but these are now currently used for spheres without any problem in accuracy or CPU time by all the scientific community involved in radiative properties calculations. We have developed our own FORTRAN codes on the basis of the subroutines proposed in the book of Bohren and Huffman (1983), and then, we are able to calculate the cross sections and the angular phase function for mono- or polydisperse spherical conducting micro-organisms (or any micro-organism considered as an equivalent sphere).

1.5 Calculation of Radiative Properties for Actual Shapes of Micro-organisms

If the previous approach is now currently used in the literature, it is limited to quasi-spherical particles corresponding to a very small part of the shape diversity in the microbial word. Moreover, if the micro-organism is not spherical, the assumption of an equivalent sphere (in surface or volume) may lead to considerable deviations in the radiative properties calculations, and consequently to strong discrepancies in the calculation of the radiation field inside the reactor (for experimental comparisons, see the next related TN 83.3). For these reasons, it is of crucial importance to develop numerical tools able to take into consideration actual shapes of micro-organisms. As already mentioned, the Lorenz-Mie approach, consisting in a variable separation method to solve the Maxwell equations has been extensively used in the 20th century in order to find exact solutions for non-spherical particles. This theoretical problem being extremely complicated, to our knowledge, until now, only two finite geometries have been extensively treated: the cylinder and, recently, the spheroid (an ellipsoid with two identical radii). Nevertheless, in the 70's, a new method called T-matrix appeared, enabling to solve this electromagnetic problem for different shapes. This integral method, based on the linearity of Maxwell equations (Mishchenko and Travis, 1998; Mishchenko *et al.*, 2000) and operating faster than the Lorenz-Mie method seems nowadays the more promising tool in solving the radiative properties of particles, mainly in the case of rotationally axi-symetric problems as previously discussed. Today, it is possible to use a free FORTRAN code, available from Mishchenko and Travis (1998), enabling to calculate the radiative properties of spheres, cylinders, spheroids and Tchebytchev particles. Unfortunately, as explained hereafter, this code is limited to small size parameters (and low asphericity) because, whatever the retained solution method, the computation becomes more difficult increasing the characteristic size or the asphericity of the particles.

1.5.1 LIMITS OF EXACT CALCULATIONS FOR ACTUAL SHAPES

For any of the two solution methods previously discussed (Lorenz-Mie or T-matrix), the computation of radiative properties of non-spherical particles becomes very tedious when increasing the size parameter and/or the asphericity of the particle. In this case, the two methods require more and more accuracy to avoid divergence, corresponding also to a strong increase in CPU calculation times. Consequently, even the more powerful approach (the T-matrix method) appears today limited by the power (and accuracy) of supercomputers to rather small particles and asphericity ratio. As an example, Table 1 gives some results obtained for prolate spheroids of increasing asphericity ratio with the best computer of the lab dedicated to numerical computation (bi-processor Xéon, 2.8 GHz). It clearly appears that the maximum equivalent size parameter available $x_{eq,v}$ strongly decreases with the asphericity ratio A_R. These results must be compared with the interesting range for photosynthetic micro-organisms. Taking practical equivalent diameters ranging between 1 and 100 µm leads to a corresponding range of 4 to 400 for size parameters. Moreover, many actual shapes of micro-organisms have asphericity ratio higher than 2 or 3 (which is the limit in using the equivalent sphere approximation); for example, this ratio is roughly 5 for *Rs. rubrum* and 50 for *A. platensis*.

In these conditions, and even if the geometrical optics approximation could be used for high values of $x_{eq,v}$, Table 1 clearly shows that the proposed rigorous T-matrix method is generally not applicable in calculating the radiative properties of most of the photosynthetic micro-organisms (for A_R = 5, the maximum size parameter is 4, corresponding to the lower limit of our practical range!). Consequently, it is necessary to develop new approximated tools enabling to work in the previous domain of interest in size parameters and for any asphericity ratio, but keeping a good accuracy in the properties computations.

Ratio between major axis *b* and minor axis *a* ($A_R = b/a$)	3/2	2	3	5	10
Maximum value of x_{eq}	50	25	10	4	3

Table 1 : Maximum values for the size (equivalent sphere in volume) parameter $x_{eq,v}$ versus the asphericity ratio A_R obtained for the calculation of radiative properties of a prolate spheroid ($b > a$) with relative refractive index m_r = 1,04 (dielectric) and with a log-normal size distribution (σ = 1,2). Results are obtained from the T-matrix code of Mishchenko and Travis (1998).

1.5.2 THE ANOMALOUS DIFFRACTION (AD) APPROXIMATION

It is possible to find a good approximation in the radiative properties calculation for micro-organisms considering that the refractive index of the particle is always close to that of the surrounding medium (i.e. water in first approximation). In this case, the relative refractive index of the particle is close to one and the Fresnel reflection coefficient tend to zero, enabling to neglect this phenomenon in the calculation of electromagnetic fields. This so-called anomalous diffraction approximation (Van de Hulst, 1981) is of crucial importance because the theoretical problem reduces to solve a scalar wave equation of Schrödinger type (this approximation is known as Schiff assumption in quantum mechanics), and then the distinction between the TE and the TM modes vanishes. Thus, defining the complex $\hat{\rho}$ (for conducting particles) or real ρ (for dielectric particles) phase shift of the wave in the particle by:

$$\boxed{\begin{gathered}\hat{\rho} = 2x\left(m_r - 1\right) = \rho\left(1 - i\tan\beta\right)\\ \rho = 2x(n_r - 1)\\ \tan\beta = \frac{\kappa_r}{n_r - 1}\end{gathered}} \qquad (38)$$

leads to the following criteria in applying the anomalous diffraction (AD) approximation:

$$\boxed{\begin{gathered}\left|m_r - 1\right| \to 0 \text{ or } \left|m_r - 1\right| << 1 \text{ and } x >> 1\\ \text{that is } n_r - 1 << 1 \text{ and } \kappa_r << 1, \text{ but for any } \hat{\rho}\end{gathered}} \qquad (39)$$

Some of these criteria are the same as the famous Rayleigh-Gans approximation (Van de Hulst, 1981), but this assumption applies only for small ρ and then practically for small size of micro-organisms, so it cannot be used for most of our applications. Conversely, the AD approximation theoretically applies for high size parameter x, but it can be shown practically that it gives very good results since $x = 1$ (Cornet – HDR), with no upper size limitation. It is then the best suitable approximation available in our case, which may lead to derive all the radiative properties of any micro-organism with a high accuracy in comparison to the exact theoretical value given by the Lorenz-Mie or T-matrix approaches (when the size parameter is sufficiently low to authorise a rigorous computation). The theoretical framework of the AD approximation has been originally established by Van de Huslt (1981) for spheres and normally illuminated cylinders, and generalised to any rotationally axi-symetric shape by Cornet (HDR). All the computations derive from the knowledge of an integral amplitude function $A(\Theta)$ which must be established for any given geometry of the particle.

1.5.3 USING THE ANOMALOUS DIFFRACTION APPROXIMATION FOR *Rs. Rubrum* OR *A. platensis* CONSIDERED AS A PROLATE CYLINDER

The non-sulphur purple photosynthetic bacteria *Rs. rubrum* has the shape of a small rod with a H/D ratio (or asphericity $A_R = b/a$) roughly equal to 4 or 5, and can then be considered as a prolate cylinder (actually, the more rigorous model of shape would be a super ellipsoid, but this geometry has not been yet treated). This assumption is also valid for the cyanobacteria *A. platensis* (A_R = 50) if the curvature radius is sufficiently high when they are spiralled. The integral amplitude function of any non-spherical particle is of course a function of the angle Θ between the incident and scattered beam of radiation but also a function of the angle θ between the axis of symmetry of the particle and the incident beam. In case of a cylinder, the general expression has been established by Cornet (HDR) and leads to the following integral of the polar angle γ:

$$\boxed{A(\Theta,\theta) = A(z_\theta,\hat{\rho}_\theta) = \int_0^{\pi/2} \left[1-\exp\left(-i\hat{\rho}_\theta \cos\gamma\right)\right]\cos\left(z_\theta \sin\gamma\right)\cos\gamma\, d\gamma} \quad (40)$$

in which we have operated the convenient variable changes and taken the definitions:

$$\boxed{\begin{aligned}
& z_\theta = x_\theta \Theta \\
& x_\theta = \frac{x_a}{\sin\theta} = \frac{2\pi\, a\, n_m}{\lambda \sin\theta} \\
& \hat{\rho}_\theta = \frac{\hat{\rho}_a}{\sin\theta} = 2x_\theta(m_r - 1) = \rho_\theta(1 - i\tan\beta) \\
& \rho_\theta = \frac{\rho_a}{\sin\theta} = 2x_\theta(n_r - 1) \\
& G_{a,\theta} = DL\, \sin\theta = 4ab\sin\theta
\end{aligned}} \quad (41)$$

The efficiencies $Q(\theta)$ can then be easily derived for the forward $\Theta = 0$ direction leading to the definitions (Cornet – HDR):

$$Q_{EXT}(\theta) = 2\,\mathrm{Re}\left\{A(0,\hat{\rho}_\theta)\right\} \quad ; \quad Q_{ABS}(\theta) = A(0, 2\rho_\theta \tan\beta) \quad (42)$$

leading finally (from eq. 21) to the mean extinction and absorption efficiencies from:

$$\boxed{\overline{Q}_{EXT} = \int_0^{\pi/2} Q_{EXT}(\theta)\sin\theta\, d\theta = 2\int_0^{\pi/2}\left[\int_0^{\pi/2}\left[1-\cos(\rho_\theta \cos\gamma)\exp\left(-\rho_\theta \tan\beta\cos\gamma\right)\right]\cos\gamma\, d\gamma\right]\sin\theta\, d\theta} \quad (43)$$

$$\boxed{\overline{Q}_{ABS} = \int_0^{\pi/2} Q_{ABS}(\theta)\sin\theta\, d\theta = \int_0^{\pi/2}\left[\int_0^{\pi/2}\left[1-\exp\left(-2\rho_\theta \tan\beta\cos\gamma\right)\right]\cos\gamma\, d\gamma\right]\sin\theta\, d\theta} \quad (44)$$

Evidently, the scattering efficiencies $Q_{SCA}(\theta)$ and $\overline{Q}_{SCA}$ can be obtained by difference between Q_{EXT} and Q_{ABS} respectively (eq. 15). In the same way, the cross sections are given by multiplying first the angular efficiencies by the angular cross-sectional area G_θ, and then averaging over all incident angles from:

$$\boxed{\overline{C}_{EXT} = 2\, DL\int_0^{\pi/2}\left[\int_0^{\pi/2}\left[1-\cos(\rho_\theta \cos\gamma)\exp\left(-\rho_\theta \tan\beta\cos\gamma\right)\right]\cos\gamma\, d\gamma\right]\sin^2\theta\, d\theta} \quad (45)$$

$$\boxed{\overline{C}_{ABS} = DL\int_0^{\pi/2}\left[\int_0^{\pi/2}\left[1-\exp\left(-2\rho_\theta \tan\beta\cos\gamma\right)\right]\cos\gamma\, d\gamma\right]\sin^2\theta\, d\theta} \quad (46)$$

the difference of which giving the scattering cross section $\overline{C}_{SCA}$.

Clearly, the relations (40-46) apply for monodisperse particles, but if a size distribution must be taken into account, a third integration given by eq. (25) is required in order to calculate the radiative properties of the polydisperse particles.

In the same way, the AD approximation authorises the calculation of the phase function for scattering. In this case, neglecting the contribution of the extremities of the cylinder, it can be shown (Van de Hulst, 1981; Cornet – HDR) that the phase function is available from the real and imaginary parts of the integral amplitude function:

$$\begin{aligned}\mathrm{Re}\{A(\Theta,\theta)\} &= \int_0^{\pi/2}\left[1-\exp\left(-\rho_\theta \tan\beta\cos\gamma\right)\cos(\rho_\theta \cos\gamma)\right]\cos\left(z_\theta \sin\gamma\right)\cos\gamma\, d\gamma \\ \mathrm{Im}\{A(\Theta,\theta)\} &= \int_0^{\pi/2}\exp\left(-\rho_\theta \tan\beta\cos\gamma\right)\sin(\rho_\theta \cos\gamma)\cos\left(z_\theta \sin\gamma\right)\cos\gamma\, d\gamma\end{aligned} \quad (47)$$

and using the definitions (eq. 16-18), to obtain the double integral averaging the polar incident angle:

$$\boxed{\overline{p_{cyl}(\Theta)} = \int_0^{\pi/2} \frac{x_a \left[\operatorname{Re}\{A(\Theta,\theta)\}^2 + \operatorname{Im}\{A(\Theta,\theta)\}^2\right]}{\pi\, Q_{SCA}(\theta)} d\theta} \quad (48)$$

As for the efficiencies and cross sections, the same remark holds on the necessity to use a third integration for polydisperse particles. Additionally, it is noteworthy that the phase function defined by eq. (48), obtained in neglecting the contribution of the extremities in the scattering process, appears only normalized in a plan perpendicular to the rotation symmetry axis, such as:

$$\boxed{\int_0^{2\pi} p_{cyl}(\Theta)\, d\Theta = 2\int_0^{\pi} p_{cyl}(\Theta)\, d\Theta = 1} \quad (49)$$

This is a crucial point because, in this form, the phase function could not be used in the source term of the RTE equation, and then requires a renormalisation over a solid angle Ω before that. This renormalisation must be performed as follows (Cornet – HDR):

$$p(\Theta) = \frac{p_{cyl}(\Theta)}{2\pi \int_0^{\pi} p_{cyl}(\Theta) \sin\Theta\, d\Theta} \approx \frac{p_{cyl}(\Theta)}{2\pi \sum_{i=1}^{2N} p_{cyl}(\Theta_i)\, w_i} \quad (50)$$

in which the integral must be evaluated by different means depending of the required accuracy. This last point is far to be trivial because the phase functions may vary in Θ by 10 orders of magnitude with strong oscillations for high size parameter, and in this case, it is not possible to use classical numerical methods or a Gaussian quadrature method.

For all the relations given by the AD approximation (eq. 40-50), we have developed Matlab® codes enabling to compute the radiative properties of monodisperse or polydisperse dielectric or conducting randomly oriented cylindrical particles. These codes are particularly useful in relation with *Rs. rubrum* and *A. platensis*, which are quasi-cylindrical micro-organisms. It must be pointed out that the computation of the functions appearing in eq. (40-50) may becomes very tedious in increasing the size parameter x or the phase shift ρ. This is mainly the case for the computation of the phase function, which requires special attention in the evaluation of integrals (47). For high size parameters (*A. platensis*), the required accuracy reaches the limit of the Matlab® software possibilities and it becomes impossible to work with the current routines for integral evaluation. Clearly, in this case, the CPU time increases dramatically, mainly if a size distribution is used, but the computation is always possible (increasing the power of the computer) at the opposite of the T-matrix method. Finally, using the optical properties and sizes of photosynthetic micro-organisms, the validity of the AD approximation has been extensively verified in comparison with the exact methods (Lorenz-

Mie and T-matrix) in the sharp domain of size parameters where they can be used. The results reveal very good agreements enabling to conclude that the AD approximation is the only way to accurately compute the radiative properties of photosynthetic micro-organisms in all the practical range in size parameters discussed above. For this reason, using the AD approximation, we have also developed Matlab® codes for the computation of radiative properties of micro-organisms with other shapes. Today, we are able to treat geometries such as spheres, spheroids, cylinders and Tchebytchev particles (i.e. spheres deformed by Tchebytchev polynomial leading to a great variety of shapes), and super ellipsoids are under investigations. These codes have been applied to very different micro-organisms of interest for the lab (or at request of other interested lab) such as bacteria (*Pseudomonas*), photosynthetic bacteria (*Rhodospirillum*, *Rhodopseudomonas*), cyanobacteria (*Arthrospira*), eukaryotic micro-organisms (*Saccharomyces*), and microalgae (*Chlamydomonas*, *Dunaliella*).

2 THE RADIATIVE TRANSFER EQUATION IN CARTESIAN AND CURVILINEAR ONE-DIMENSIONAL GEOMETRIES

2.1 *Overview of the radiative transfer problem in one-dimensional geometries*

It is well known that radiative transfer applications are by nature three-dimensional problems. Nevertheless, in the field of photobioreactors, the one-dimensional approximation can often be used, depending mainly of the geometric arrangement of the pair reactor / lightening system. This requires of course being able to quantify accurately the incident light flux density $q_\cap$ as pseudo-homogeneous on the illuminated area of the PBR by theoretical or experimental tools whereas it is generally locally heterogeneous. Moreover, the one-dimensional attenuation of light inside the reactor, enabling to control easily the field of radiation, is probably one of the more important criteria in designing new PBR of the future, with high productivities. Consequently, modelling the one-dimensional light transfer inside vessels of different geometries appears as a point of crucial importance, not only because this assumption corresponds to most of the PBR used in the MELiSSA team.

If the one-dimensional radiative transfer problem in Cartesian geometries has been extensively studied in the past decades (Siegel and Howell, 2002), it is far to be the case in curvilinear systems of coordinates (Heaslet and Warming, 1966; Thynell, 1989). This comes from the facts that first, these geometries (mainly the cylindrical one) does not present any interest in different fields of theoretical physics involved in radiative transfer problems (as for example astrophysics…), and second, curvilinear coordinates lead to a higher mathematical complexity for a problem which is already complicated in rectangular geometry. Particularly, the curvilinear geometry (cylindrical or spherical) implies axi-symetric problems, which are known to induce strong difficulties in finding solutions at the centre of the considered volume.

In this Technical Note, the authors propose to develop a general and innovative methodology enabling to treat directly all the three one-dimensional systems of coordinates from a unified way. This corresponds to the rigorous treatment of a previous tentative (Cornet *et al.*, 1995) which have only led to approximate solutions in curvilinear coordinates as explained in TN 55.1 (Cornet *et al.*, 2005), mainly for cylindrical systems.

First of all, to thoroughly understand this method, it is necessary to discuss the mathematical nature of the transport equation operator. In pseudo steady-state conditions, this is a five Euclidean operator, the parameters of which can be divided in two categories:

- ✓ Parameters depending on the system geometry
- ✓ Parameters independent from the considered geometry

2.1.1 PARAMETERS DEPENDING ON THE SYSTEM GEOMETRY

These parameters are those of the position vector, i.e. the coordinates defining this vector and the vectorial base for the considered geometry. They are schematized in the following table:

Cartesian system	**Cylindrical system**	**Spherical system**
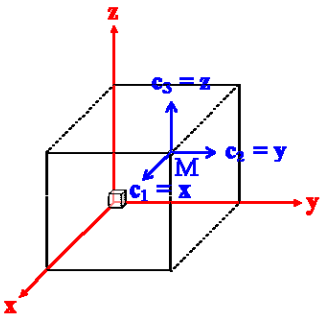	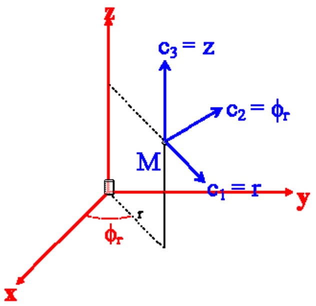	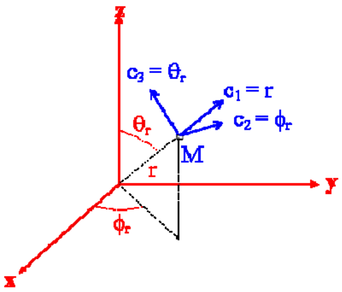
3 abscissas (x, y, z)	2 abcissas (r, z) + 1 angle (ϕ_r)	1 abscissa (r) + 2 angles (ϕ_r, θ_r)
m = 0	***m = 1***	***m = 2***

In this table, two kinds of reference frame can be distinguished: a fixed frame (O,x,y,z) and a mobile one (M,c_1,c_2,c_3). The value of *m*, in the last line of the table, is the number of angles that composes the coordinates of the position vector. This value is of fairly importance to formulate a universal operator in one-dimensional systems.

2.1.2 PARAMETERS INDEPENDENT FROM THE GEOMETRY

These parameters are defined in the mobile frame of reference (M,c_1,c_2,c_3). Consequently, the definitions do not vary whatever the geometry might be.
Firstly, a unitary directional vector must be defined to formulate the operator of radiative transfer equation. This vector will be denoted $\mathbf{\Omega}$.

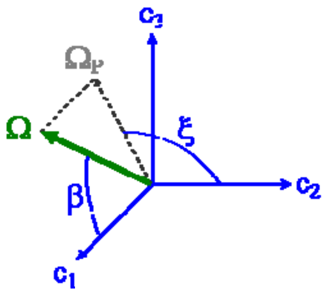

This $\mathbf{\Omega}$ vector allows defining every physical variable of interest for the radiative transfer problems. Its coordinates depend on two angles, denoted β et ξ and representing respectively the zenith and the azimuth of the vector in relation to the coordinate c_1, which will be considered as the key-coordinate.

The main related variables are the radiant intensity I_λ, the radiant flux density q_λ and the irradiance G_λ. These three variables are spectral values (in USI.m^{-1}), but can be integrated over a given range of wavelength to obtain mean values in a considered domain of interest.

- ✓ Intensity : The unit of spectral radiant intensity is W.m^{-2}.sr^{-1}.m^{-1}. This is a variable, which depends on the coordinates of the position vector M (c_1, c_2, c_3) and on the direction of the unitary vector $\mathbf{\Omega}$ (β, ξ). It is then a function depending on five variables. However, in the cases of interest for us, it will be quite easy to demonstrate that spectral intensity is independent from two coordinates and from azimuth (because of the symmetry). Then, the intensity can be considered as varying only with one coordinate and one angle: I_λ = f (c_1, β). This physical quantity represents the energy flux, which arrive from direction $\mathbf{\Omega}$ to an observer, by unit of solid angle.

- ✓ Radiant flux density and irradiance : These variables are integral values over a 4π solid angle, expressed in W.m^{-2}.m^{-1}. Their angular nature depends on the field of radiation hypothesis in the photobioreactor.

2.1.3 THE RADIATIVE TRANSFER (OR PHOTON TRANSPORT) EQUATION

Once the radiative properties of the medium are known (part 1), it is then possible to derive the universal one-dimensional form of the radiative transfer equation (RTE) from the previously defined variables and key parameters. This requires first to simplify the general three-dimensional form of the RTE for a non-emissive, scattering and participating medium, which is in fact a photon transport equation, so formulated:

$$\nabla \cdot (\mathbf{\Omega} I_\lambda) = -(a_\lambda + s_\lambda) I_\lambda + \frac{s_\lambda}{4\pi} \int_{\beta'=0}^{\pi} \int_{\xi=0}^{2\pi} I'_\lambda \, p_\lambda(\mathbf{\Omega},\mathbf{\Omega}') \sin\beta' d\beta' d\xi' \qquad (51)$$

where a_λ and s_λ are respectively the absorption and scattering volumetric coefficients of the particles. The integral term is a collision integral (photon scattering is considered as elastic in the medium) characterised by the phase function p_λ ($\mathbf{\Omega}$,$\mathbf{\Omega}$'). From our previous notations, expressing a universal operator (left term) for standard systems of coordinates is then possible. This operator depends mainly on the number of angles defining the geometry, m, as introduced above, and the following unified expression is obtained:

$$\nabla \cdot (\mathbf{\Omega} I_\lambda) = \mathbf{\Omega} \cdot \nabla I_\lambda = \frac{dI_\lambda}{dc_1}\cos\beta + \frac{\sin\beta\cos\xi}{c_1^{\left(\frac{m(3-m)}{2}\right)}}\frac{dI_\lambda}{dc_2} + \frac{\sin\beta\sin\xi}{(c_1\sin c_2)^{\left(\frac{m(m-1)}{2}\right)}}\frac{dI_\lambda}{dc_3} \qquad (52)$$

It can be formulated of course, assuming the one-dimensional hypothesis, whatever the system of coordinates might be (rectangular, cylindrical or spherical) giving (Van Noort, 2002):

$$\nabla^{\circ} \cdot (\mathbf{\Omega} I_\lambda) = \frac{dI_\lambda}{dc_1}\cos\beta \qquad (53)$$

enabling to develop universal method in solving the one-dimensional form of the RTE.

2.2 The generalised two-flux method approximation

The two-flux method is probably the easiest method to solve the RTE. It uses considerable simplifying assumptions but enables to derive very practical analytical expressions of physical variables characterising the state of radiations in a considered system. It has been used extensively in the early stage of the MELiSSA project (Cornet *et al.*, 1992; 1995; 1998), using a diffuse and isotropic assumption for the radiation field and so defining empirically radiative properties for micro-organisms requiring an experimental determination with the opalescent plate method of Aiba (1982). Considering now exact radiative properties of micro-organisms (including exact phase function for scattering), the problem will be rigorously and properly reformulated in the following.

Let's remind first the principle of the two-flux method: It consists in dividing space in two complementary hemispheres, where intensities have to be assumed angular independent (or easily mathematically expressible). The hemisphere defined by acute zeniths (positive cos$\beta \in [0, \pi/2]$) is named positive hemisphere. Negative hemisphere is of course the complementary hemisphere (obtuse zeniths, negative cos$\beta \in [\pi/2, \pi]$). In fact, the radiative transfer problem strongly depends on the angular nature of the field of radiation at the boundaries and inside the PBR. Generally speaking, the angular distributions of the field at the boundaries (fixed by the lightening system), and inside the reactor (fixed by the radiative properties of the material phase) are not the same. In this case, it is necessary to treat the problem of discontinuity at the boundaries, and consequently, the radiative transfer problem appears non-linear, even for constant radiative properties of the medium. This requires then developing sophisticated high order numerical tools, as they will be presented later in this TN (part 2.3).

Nevertheless, if the assumption is made to consider a linear problem, i.e. if the angular nature of the radiation fields outside and inside the PBR are taken to be the same and independent by any way from the angles β and ξ, it is then possible to simplify considerably the light transfer problem applying the two-flux method which gives rise in many cases to an analytical solution. Conversely, the availability of this method is limited by the fact that only two simple hypotheses relative to the angular independence of the intensities exist: respectively the diffuse and collimated field of radiation. This is the reason why the two-flux method appears as a good approximation only if there is a close agreement between the incident angular distribution of the radiation field and the phase function for scattering inside the medium (e.g. a collimated incident radiation with a highly forward phase function of micro-organisms). Analytical expression for flux and irradiance in the PBR are thus conditioned by the radiation hypothesis. Although a diffuse radiation field was formerly assumed, the collimated radiation field assumption is now considered as more relevant for most practical lightening devices. Fortunately, the phase functions for scattering of *Rs. Rubrum* or *A. platensis* are more collimated than diffuse. In all cases, the two ways in obtaining intensities independent from the solid angle Ω and their mathematical treatment for the generalised two-flux method are summarised on the following scheme.

Diffuse hypothesis	***Collimated hypothesis***
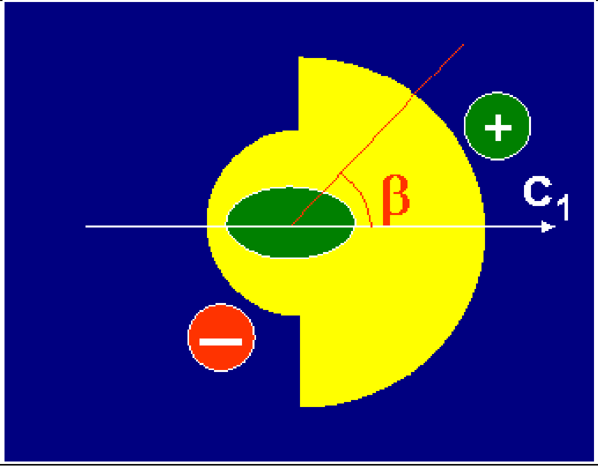	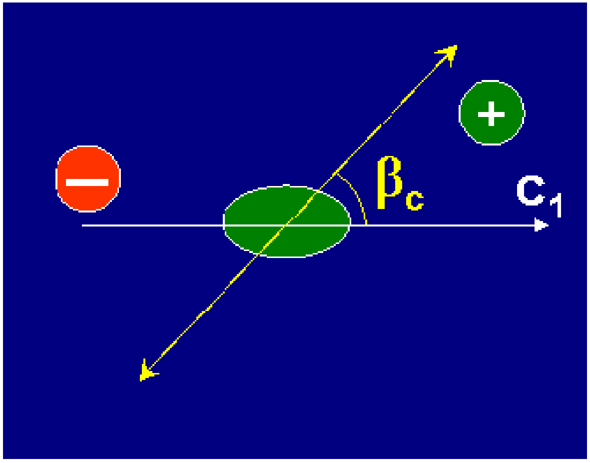
$\cos(\beta) > 0 \Rightarrow I_\lambda = I_\lambda^+$ $\cos(\beta) < 0 \Rightarrow I_\lambda = I_\lambda^-$	$\cos(\beta) > 0 \Rightarrow I_\lambda = \delta_{\beta=0} I_\lambda^+$ $\cos(\beta) < 0 \Rightarrow I_\lambda = \delta_{\beta=\pi} I_\lambda^-$ with $\delta_{\beta=\beta c}$ Krönecker delta

Finally, two half-equations, defined on positive and negative hemispheres, can be obtained by part integration of RTE on each hemisphere, depending of assumption chosen to have independent intensities (diffuse or collimated):

	Diffuse hypothesis	Collimated hypothesis

Positive hemisphere	$\frac{dI_\lambda^+}{dc_1} = -2a_\lambda I_\lambda^+ - 2\bar{b}_\lambda s_\lambda \left(I_\lambda^+ - I_\lambda^-\right)$ (54a)	$\frac{dI_\lambda^+}{dc_1} = -a_\lambda I_\lambda^+ - \bar{b}_\lambda s_\lambda \left(I_\lambda^+ - I_\lambda^-\right)$ (54b)
Negative hemisphere	$\frac{dI_\lambda^-}{dc_1} = 2a_\lambda I_\lambda^- - 2\bar{b}_\lambda s_\lambda \left(I_\lambda^+ - I_\lambda^-\right)$ (55a)	$\frac{dI_\lambda^-}{dc_1} = a_\lambda I_\lambda^- - \bar{b}_\lambda s_\lambda \left(I_\lambda^+ - I_\lambda^-\right)$ (55b)

where $\bar{b}_\lambda$ is the backward scattered fraction, obtained by integration of the exact phase function (see part 1) as $\bar{b}_\lambda = \frac{1}{2}\int_{\frac{\pi}{2}}^{\pi} p_\lambda(\beta,\beta')\sin\beta\, d\beta$.

It must be noted that these equations are each defined **solely** on one hemisphere. Consequently, these pair of equations are mathematically defined on two half open surfaces and not rigorously on a closed surface, as it should be to verify the Gauss divergence theorem. Furthermore, with our system of notation, these half-equations being the same in the three systems of coordinates, the analytical solutions obtained should be the same in cylindrical and rectangular systems, which is of course incorrect. The bias comes from the fact that this system is only self consistent in Cartesian system of coordinates for which there is no difference in the one-dimensional operators' gradient and divergence. In the general case (mainly in curvilinear coordinates), the two half-equations each defined on one hemisphere are not sufficient to find physical variables (as irradiance or flux density) defined on the entire space (the 4π solid angle *Ω*), but having two unknowns I_λ^+ and I_λ^-, it is necessary to provide two equations defined on this entire space.

The first equation is obtained by summing the two half-equations of the previous system:

$$\frac{\partial\left(I_\lambda^+ + I_\lambda^-\right)}{\partial c_1} = -k_h(a_\lambda + 2\bar{b}_\lambda s_\lambda)\left(I_\lambda^+ - I_\lambda^-\right) \qquad (56)$$

where $k_h = 1$ for a collimated field of radiation, and $k_h = 2$ for a diffuse radiation field.

The second equation is introduced to verify *per se* the closed surface of integration, because integrating the RTE (eq. 51) over 4π steradians and applying the Gauss divergence theorem leads to the well-known local balance of radiant energy for the photonic phase (Cornet *et al.*, 1995 and 1998):

$$\nabla\cdot\mathbf{q}_\lambda = -a_\lambda G_\lambda \qquad (57)$$

This equation of radiant energy conservation, which relies the irradiance to the divergence of the radiative flux, must be of course satisfied in all points of the system. From the independent variables and parameters previously defined in the proposed unified view, the one-dimensional form of this equation becomes for any system of coordinates:

$$\frac{\partial\left(I_\lambda^+ - I_\lambda^-\right)}{\partial c_1} + \frac{m}{c_1}\left(I_\lambda^+ - I_\lambda^-\right) = -k_h a_\lambda \left(I_\lambda^+ + I_\lambda^-\right) \qquad (57')$$

The differential system obtained (eq. 56 and 57') can be solved very easily by differentiating the first equation and combining it in the second equation. A second-degree differential equation is then appearing. This characteristic equation describes completely the system and is written as follows:

$$\frac{\partial^2\left(I_\lambda^+ + I_\lambda^-\right)}{\partial c_1^2} + \frac{m}{c_1}\frac{\partial\left(I_\lambda^+ + I_\lambda^-\right)}{\partial c_1} - k_h{}^2 a_\lambda (a_\lambda + 2\bar{b}_\lambda s_\lambda)\left(I_\lambda^+ + I_\lambda^-\right) = 0 \qquad (58)$$

A new formalism can be substituted by combining the definition of irradiance with the characteristic equation:

$$G_\lambda = \int_{4\pi} I_\lambda d\Omega = k_h \pi^{k_h - 1}(I_\lambda^+ + I_\lambda^-) \qquad (59)$$

$$\frac{\partial^2 G_\lambda}{\partial c_1^2} + \frac{m}{c_1}\frac{\partial G_\lambda}{\partial c_1} - k_h{}^2 a_\lambda (a_\lambda + 2\bar{b}_\lambda s_\lambda) G_\lambda = 0 \qquad (60)$$

This kind of differential equation is mathematically well-known and analytical solutions, depending on the parameter *m* and on boundary conditions can be calculated.

In this work, the following boundary conditions will be used:

- ✓ Rectangular system (*m* = 0): A rectangular vessel enlightened on one face will be considered, the c_1 direction being the perpendicular direction to the enlightened face. In this case, the boundary conditions are:
  $I_\lambda^+(c_1 = 0) = I_{\lambda,\cap}$, with $I_{\lambda,\cap}$ an imposed constant.
  $I_\lambda^-(c_1 = L) = 0$, with L being the path length (involving no reflection for c_1=L).

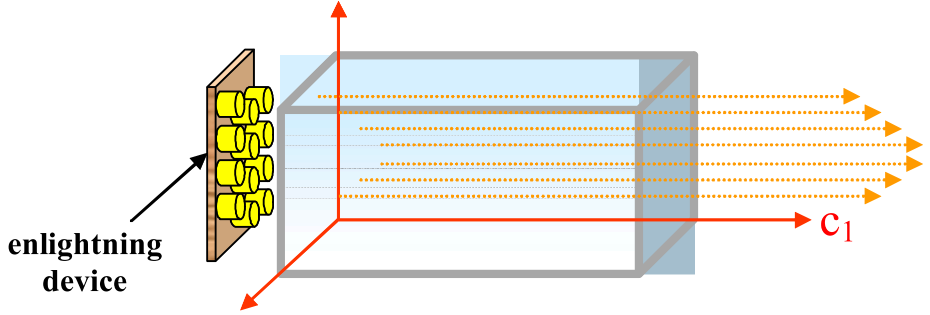

This kind of geometry corresponds to some PBR systems, but mainly to spectrophotometers or optical bench with integrating sphere.

- ✓ Cylindrical system ($m = 1$): A cylindrical PBR, radially enlightened will be considered. The first boundary condition for $c_1 = R$ (the radius of the PBR) is similar to the first condition formulated in rectangular system, but for the negative hemisphere:
  $I_\lambda^-(c_1 = R) = I_{\lambda,\cap}$.
  The second condition is imposed by the geometry of the system, indeed the symmetry existing for $c_1 = 0$ induces the following relations:
  $I_\lambda^+(c_1 = 0, \phi_{r0}) = I_\lambda^+(c_1 = 0, \phi_{r0} + \pi) = I_\lambda^-(c_1 = 0, \phi_{r0})$
  which implies: $q_\lambda(c_1 = 0) = \pi^{k_h - 1}\left(I_\lambda^-(c_1 = 0) - I_\lambda^+(c_1 = 0)\right) = 0$.

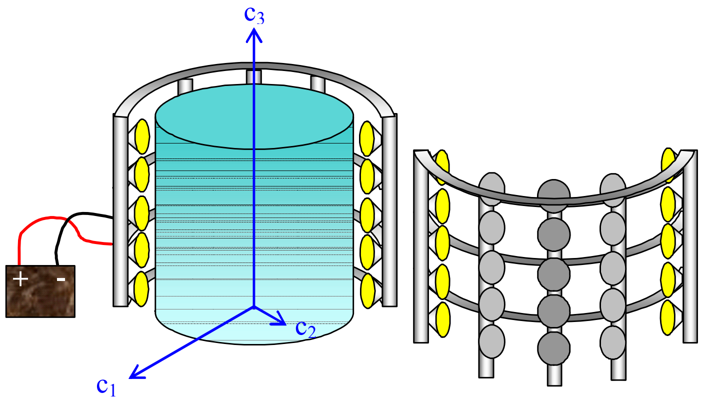

- ✓ Spherical system ($m = 2$): A sphere enlightening space around it will be considered. The following boundary conditions will then be used:
  $I_\lambda^+(c_1 = r_s) = I_{\lambda,\cap}$, with r_s the sphere radius.
  $I_\lambda^-(c_1 = \infty) = 0$

For these three practical cases, the analytical solutions obtained for the characteristic equation (60) are summarized in the following tables. Moreover, the profiles solutions are plotted in Appendix 2 for the two formers.

	Relative Irradiance $\frac{G_\lambda}{q_{\lambda,\cap}}$
rectangular symmetry (m = 0)	$2k_h \frac{\sinh\left(\delta_\lambda (L-x)\right) + \alpha_\lambda \cosh\left(\delta_\lambda (L-x)\right)}{2\alpha_\lambda \cosh\left(\delta_\lambda L\right) + (1+\alpha_\lambda^2)\sinh\left(\delta_\lambda L\right)}$ (61a)
cylindrical symmetry (m = 1)	$2k_h \frac{I_0(\delta_\lambda r)}{I_0(\delta_\lambda R) + \alpha_\lambda I_1(\delta_\lambda R)}$ (61b)
spherical symmetry (m = 2)	$2k_h \frac{r_s^2}{r^2}\left(\frac{\delta_\lambda r}{\delta_\lambda r_s + \alpha_\lambda (1+\delta_\lambda r_s)}\right)\exp(-\delta_\lambda (r - r_s))$ (61c)

	Relative flux density $\frac{q_\lambda}{q_{\lambda,\cap}}$
rectangular symmetry (m = 0)	$2\alpha_\lambda \frac{\cosh\left(\delta_\lambda (L-x)\right) + \alpha_\lambda \sinh\left(\delta_\lambda (L-x)\right)}{2\alpha_\lambda \cosh\left(\delta_\lambda L\right) + (1+\alpha_\lambda^2)\sinh\left(\delta_\lambda L\right)}$ (62a)
cylindrical symmetry (m = 1)	$-2\alpha_\lambda \frac{I_1(\delta_\lambda r)}{I_0(\delta_\lambda R) + \alpha_\lambda I_1(\delta_\lambda R)}$ (62b)
spherical symmetry (m = 2)	$2\alpha_\lambda \frac{r_s^2}{r^2}\left(\frac{(1+\delta_\lambda r)}{\delta_\lambda r_s + \alpha_\lambda (1+\delta_\lambda r_s)}\right)\exp(-\delta_\lambda (r - r_s))$ (62c)

In these solutions, the two important parameters α_λ and δ_λ are defined as follows:

$$
\begin{aligned}
&\alpha_\lambda = \sqrt{\frac{Ea_\lambda}{Ea_\lambda + 2\bar{b}_\lambda Es_\lambda}} \\
&\delta_\lambda = k_h C_X \sqrt{Ea_\lambda \left(Ea_\lambda + 2\bar{b}_\lambda Es_\lambda\right)} \\
&\text{that is :} \qquad\qquad\qquad\qquad\qquad\qquad (63) \\
&\delta_{c,\lambda} = C_X \sqrt{Ea_\lambda \left(Ea_\lambda + 2\bar{b}_\lambda Es_\lambda\right)} \\
&\delta_{d,\lambda} = 2C_X \sqrt{Ea_\lambda \left(Ea_\lambda + 2\bar{b}_\lambda Es_\lambda\right)}
\end{aligned}
$$

The spectral parameter δ_λ is the general extinction coefficient for the two-flux method, whereas the linear scattering modulus α_λ quantifies the respective part of absorption and scattering by the medium (α_λ = 1 for a perfect absorptive medium and α_λ = 0 for a perfect scattering medium). This parameter is more significant than the albedo for scattering because it takes into account the effect of the phase function on the scattering phenomenon from the backward scattered fraction $\overline{b}_{\lambda}$. For example, using the exact radiative properties for *Rhodospirillum rubrum* at 350 nm, the calculation of the albedo gives $\omega_{350} = 0.931$ (perfect scattering is reached at ω = 1) and $\alpha_{350} = 0.990$. This last value means that *Rs. rubrum* presents rather an absorptive behaviour at this wavelength, whereas the value of the albedo seems indicating a scattering behaviour, neglecting the effect of the phase function which is sharply peaked in the forward direction for micro-organisms.

2.3 THE GENERAL DIFFERENTIAL DISCRETE ORDINATES METHOD

As previously explained, the two-flux method provides only an approximate solution for the RTE. In many practical cases, the accuracy of this method is not sufficient because it gives only a rough description of the radiation field, mainly interesting for non-linear model based predictive control of PBR requiring a fast estimate of the process output. Particularly, understanding and predicting the very complex sub-critical bifurcation appearing in continuous cultivation of the purple bacteria *Rs. rubrum* (Cornet *et al.*, 2005 – TN 55.1) requires to obtain more accurate solutions of the RTE to be sure of the appearance of the physical light-limited regime and of the value of the working illuminated fraction. It is then necessary to develop more sophisticated numerical tools in order to obtain an exact solution for the one-dimensional form of the RTE. Among the existing methods in the literature (Mengüç and Viskanta, 1983; Siegel and Howell, 2002), the P_N method of moments (or spherical harmonics method), and the F_N methods require to work with Legendre polynomials even for the phase function of the particles, thus it is not possible to use the exact radiative properties developed in the first part of this TN in these cases. At the opposite, the discrete ordinate method that may be differential (d-S_N) or algebraic (S_N), requiring to choose *a priori* a given number of known ordinates appears as the best candidate method. In this work, the differential discrete ordinates (d-S_N) method will be used to calculate flux densities and irradiances in the PBR. This numerical method, originally proposed by Chandrasekhar (1960), is based on a simple quadrature concept (Ramkrishna and Amundson, 2004). It permits to discretise an integral term, i.e. to transform it in a sum of finite terms.

$$\int_0^{\pi} f(\beta)\sin\beta\, d\beta = \sum_{i=1}^{2N} w_i\, f(\beta_i) \qquad (64)$$

The quadrature is represented by a set of couples (w_i, β_i). Two quadratures are widespread: the Gauss quadrature (Davis and Rabinowitz, 1956) and the Lobatto quadrature (Michels, 1963). The Lobatto quadrature will be used in this note because it presents a particular couple for $\beta = 0$ which is particularly convenient in case of collimated incidences.

The method, which is hereafter described, is a generalisation of the method proposed by Kumar *et a*l. (1990). This generalisation is of crucial importance for our purposes because first, it enables to work with the actual phase function (instead of a smoothed series of Legendre polynomials leading to a poor estimate for the more significant angles below π/4), and second, it can be used in any Cartesian or curvilinear coordinates. In any way, the principle of the method is to work on a discretised radiative transfer equation as follows:

$$\begin{aligned} &\frac{dI_\lambda(\beta)}{d\tau}\cos\beta = -I_\lambda(\beta) + \frac{\omega_\lambda}{2}\int_0^\pi p_\lambda(\beta,\beta')I_\lambda(\beta')\sin\beta' d\beta' \\ \Rightarrow &\frac{dI_\lambda(\beta_i)}{d\tau}\cos\beta_i = -I_\lambda(\beta_i) + \frac{\omega_\lambda}{2}\sum_{k=1}^{N} p_\lambda(\beta_i,\beta_k)w_k I_\lambda(\beta_k) \end{aligned} \qquad (65)$$

To maintain a good ratio between accuracy and calculation time, the number of ordinates *N* will be fixed to 32, according to Kumar *et al.* (1990). This method will thus be denoted d-S_{32} method (or DDO_{32} for Kumar *et al.*). Nevertheless, it should be kept in mind that the general reference method (giving in all cases exact results for the solution of the RTE) will be the d-S_{96} method. This method however is rarely used (except for example if the objective of a calculation is to validate first the radiative properties by comparison with experimental measurement using an integrating sphere photometer) because the calculation time can become prohibitive.

2.3.1 MANAGING THE SYSTEM OF EQUATIONS

To simplify and generalise the formulation of the equation system (65), several new notations have been used.
First, the albedo of single scattering was introduced as:

$$\omega_\lambda = \frac{Es_\lambda}{Ea_\lambda + Es_\lambda}. \quad (66)$$

Resulting in the appearance of the reduced coordinate, the so-called optical thickness, defined in any system of coordinate by :

$$\tau_1 = \left[(Ea_\lambda + Es_\lambda)C_X\right]c_1. \quad (67)$$

Ultimately, the cosine of the zenith β_i will be denoted $\mu_i = \cos\beta_i$.

The discretised radiative transfer equation (eq. 65) then becomes:

$$\frac{dI_{i,\lambda}}{d\tau_1}\mu_i = -I_{i,\lambda} + 2\pi\omega_\lambda \sum_{k=1}^{N} P_{(i,k),\lambda} w_k I_{k,\lambda} \qquad (68)$$

in which $I_{i,\lambda}$ is the spectral intensity for angle β_i and $P_{(i,k),\lambda}$ is a matrix describing the actual phase function for scattering with wavelength λ (see part 1). It must be noticed that the appearance of the term 2π just corresponds to a change in normalisation of the phase function (it is normalised to 1 with the Lorenz-Mie theory instead of 4π in the field of radiative transfer). The 32 equations may then be written as an array:

$$\frac{d\mathbf{I}_\lambda}{d\tau_1} = \mathbf{M}^{-1}\left(-\mathbf{D}_\mathbf{N} + 2\pi\omega_\lambda \mathbf{P}_\lambda \mathbf{W}\right)\mathbf{I}_\lambda \qquad (69)$$

with :

- $\mathbf{I}_\lambda$: a column vector containing the spectral intensities $I_{i,\lambda}$.
- $\mathbf{M}$: a diagonal matrix with $\mathbf{M}_{i,i} = \mu_i$ and $\mathbf{M}_{i,j\neq i} = 0$.
- $\mathbf{D}_\mathbf{N}$: the N*N eye matrix.
- $\mathbf{P}_\lambda$: the full N*N spectral phase function matrix (generated by a specific Matlab® program from the theoretical results of part 1).
- $\mathbf{W}$: a diagonal matrix with $\mathbf{W}_{i,i} = w_i$ and $\mathbf{W}_{i,j\neq i} = 0$.

The above matrix equation represents the whole set of discretised equations of radiative transfer. They describe the mathematical links between a spectral intensity for one direction and the spectral intensities for all other directions. Consequently, these equations will be named Link-equations.

As previously discussed for the two-flux method, obtaining a mathematically rigorous solution is not possible in the current state of the equation system, because one equation is missing (in curvilinear coordinates). Indeed, for the moment, (N-1) intensities can be expressed in function of the last intensity. A constraint-equation is needed to superimpose the conservation principle of radiant energy on the photonic phase, which is formulated in the form:

$$\nabla \cdot \mathbf{q}_\lambda = \frac{dq_\lambda}{d\tau_1} + m\frac{q_\lambda}{\tau_1} = -a_\lambda G_\lambda = -A_\lambda \qquad (70)$$

showing that a singular term appears. It is conditioned by the number of angle in the studied system of coordinates. Using the definition of flux density and irradiance, the constraint-equation can be discretised as follows:

$$\sum_{i=1}^{N} w_i\mu_i \frac{dI_{i,\lambda}}{d\tau_1} = -(1-\omega_\lambda)\sum_{i=1}^{N} w_i I_{i,\lambda} - \frac{m}{\tau_1}\left[\sum_{i=1}^{N} w_i\mu_i I_{i,\lambda}\right] \qquad (71)$$

and from our previous notations written under the following matrix formalism:

$$\frac{d\,\mathbf{I}_\lambda}{d\tau_1} = -\left((1-\omega_\lambda)\,\mathbf{M}^{-1} + \frac{m}{\tau_1}\mathbf{D}_\mathbf{N}\right)\mathbf{I}_\lambda \qquad (72)$$

Finally, combining eq. (69) and (72) leads to a complete matricial system giving all the *N* intensities and established hereafter for the first time in a so general way:

$$\frac{d\,\mathbf{I}_\lambda}{d\tau_1} = \left[\frac{\mathbf{M}^{-1}}{N}\left[(N-1)\left(-\mathbf{D}_\mathbf{N} + 2\pi\,\mathbf{P}_\lambda\mathbf{W}\right) - (1-\omega)\,\mathbf{D}_\mathbf{N}\right] - \frac{m}{N\,\tau_1}\mathbf{D}_\mathbf{N}\right]\mathbf{I}_\lambda \qquad (73)$$

This differential system can be solved with Matlab® assuming either collimated or diffuse radiation hypotheses at the boundaries. Some examples of solutions are plotted in appendix 3. The use of a high order quadrature and of a **P** matrix with actual phase function of micro-organisms conjugated with exact values for the absorption and scattering coefficients appearing in the optical thickness τ_1 and in the albedo of single scattering ω_λ guarantees to obtain exact solutions to the one-dimensional radiative transfer problem in any geometry of PBR. It must be pointed out that (in the limit of our knowledge of the literature) a so refined technique, enabling to solve accurately the RTE with actual radiative properties of particles, has never been published before in any field of the physicists' community in connexion with the equation of transport.

2.3.2 CALCULATION TIME

As already mentioned, depending on the order of the quadrature, the calculation time to obtain flux density and irradiance with Matlab® can vary dramatically. The calculation time is then an important parameter, which must be dealt with before starting working with numerical method. Parameters that may influence calculation time are:

- Quadrature order
- Optical thickness
- Albedo number
- Points per profile (PPP)

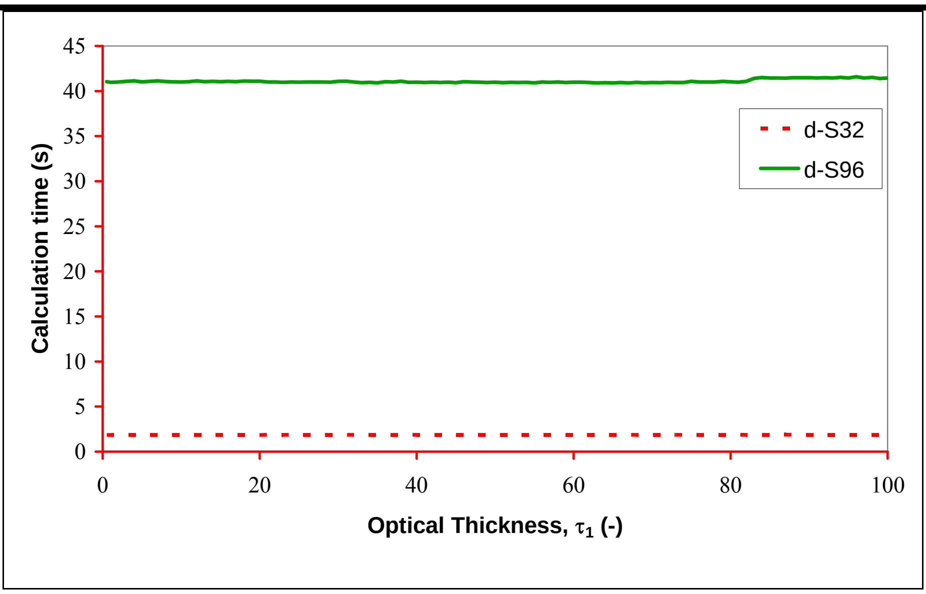

Figure 1: Influence of the optical thickness τ_1 on d-S_n method's calculation time. Full line and dashed line respectively correspond to d-S_{96} and d-S_{32} method. Calculations were performed considering a diffuse radiation field, a typical albedo number ω = 0.90 and 100 points per profile.

2.3.2.1 Quadrature order and optical thickness

Profiles of flux density and irradiance were calculated for optical thicknesses from 0 to 100, using d-S_{32} and d-S_{96} methods. As it can be seen on Figure 1, optical thickness seems having no influence on calculation time. At the contrary, the quadrature order plays a crucial role and the d-S_{96} method needs a calculation time 20 times more important than the d-S_{32} method on this example. It must be pointed out first that this ratio is strongly influenced by the radiative properties of the medium, and second that the independence of the optical thickness is a specificity of the Matlab® routine used to solve the two points boundary values problem, because using a Fortran code with a shooting point method displays a dramatic effect of this parameter on the computation time.

2.3.2.2 Quadrature order and albedo

As it can be seen on Figure 2, calculation time seems to be independent from the albedo number. This feature is also a benefit of the Matlab® routine used.

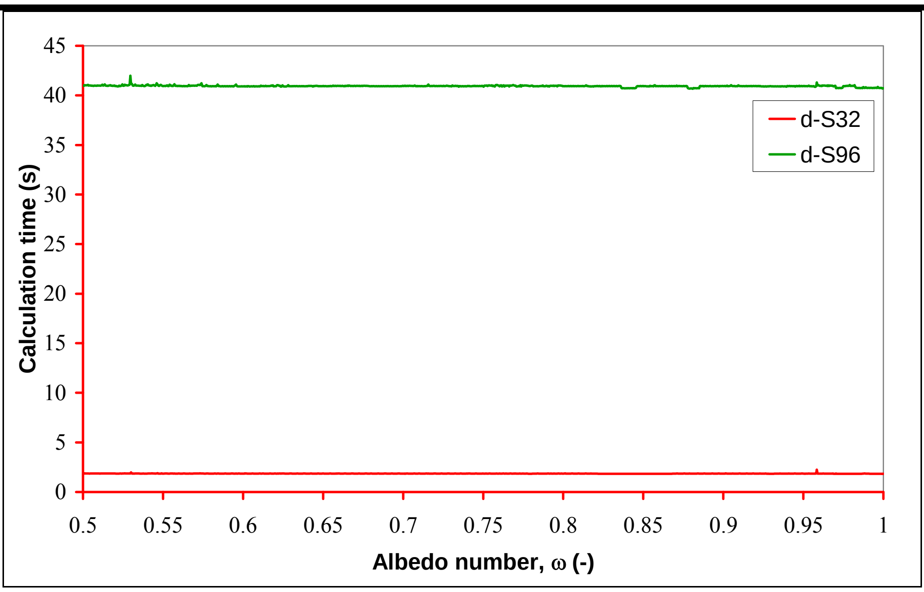

Figure 2: Influence of the albedo number ω on d-S_n method's calculation time. Full line and dashed line respectively correspond to d-S_{96} and d-S_{32} method. Calculations were performed considering a diffuse radiation field, an optical thickness τ_1 = 10 and 100 points per profile.

2.3.2.3 *Points per profile (PPP)*

Evidently, using the d-S_N method with Matlab® requires to define calculation parameters like the number of points per profile. This PPP-number quantifies the resolution enabling to discriminate two nearby local fluxes.

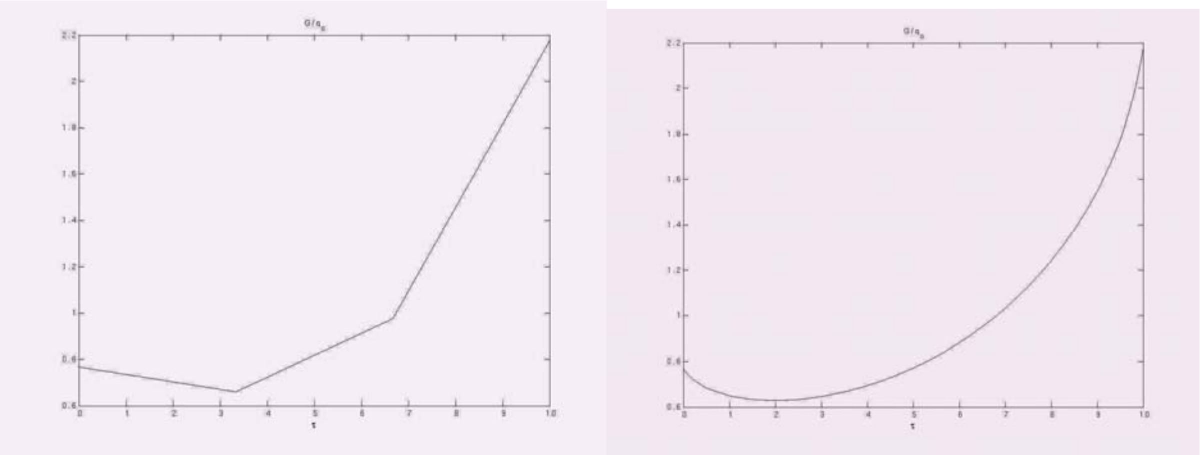

For example, on the scheme above, a comparison is made with an irradiance profile calculated in a cylindrical PBR obtained with the d-S_{32} method. On the left, the PPP-number was set to 4, whereas on the right, the same profile with PPP-number set to 100 was drawn.

It can be seen easily that the calculation time strongly depends on this parameter. Taking values of PPP-number ranging between 3 to 1000 gives results plotted on Figure 3, showing that calculation time (work station, AMD Xeon bi-processor, 2.8 Ghz) increases as the square of the PPP-number. On this figure obtained with the d-S_{96} method, the calculation times becomes significant for a high number of points per profile (2220 seconds at PPP = 1000), nevertheless, it must be kept in mind that for the same case, using the lower accurate d-S_{32} method leads to very reasonable values (85 seconds for PPP = 1000).

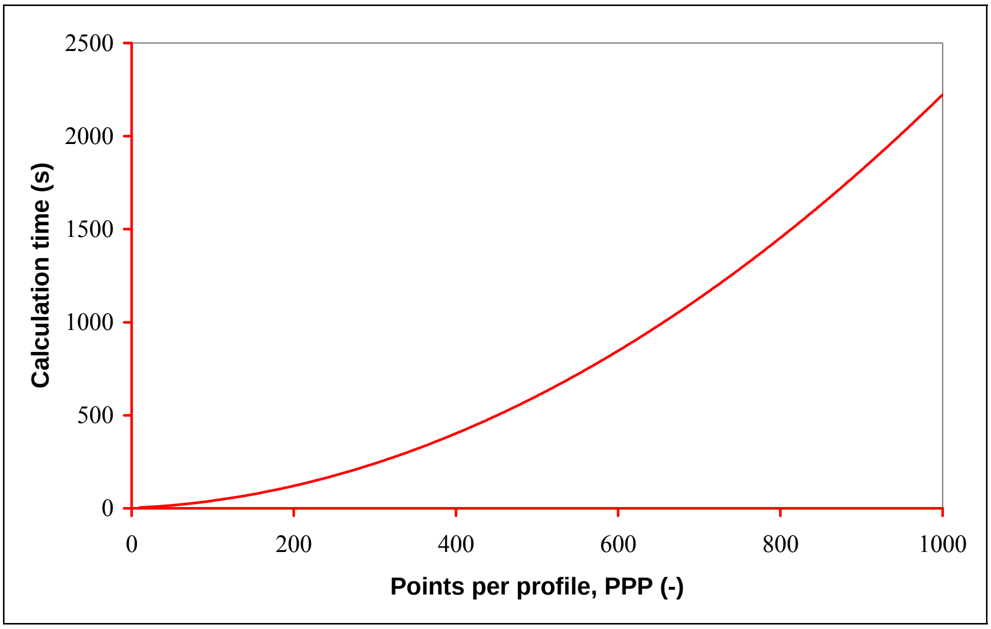

Figure 3: Influence of the number of points per profile *PPP* on d-S_{96} method's calculation time. Calculations were performed considering a diffuse radiation field, an optical thickness τ_l = 10 and an albedo number ω = 0.90.

3 INFLUENCE OF RADIATIVE PROPERTIES AND METHODS IN SOLVING THE RADIATIVE TRANSFER EQUATION

In the first part of this TN, we have presented and discussed two general methods enabling the calculation of the radiative properties of a given micro-organism, either from a classical Lorenz-Mie approach considering the particle as an equivalent sphere (generally used in the literature), either from an original new method developed at LGCB and using the actual shape of the particle with the anomalous diffraction assumption. In the second part, we discussed two different methods in solving the RTE itself, once the radiative properties are known; a generalised two-flux method which remains an important simplification of the mathematical problem and leads in many cases to analytical solutions, and a generalised differential discrete ordinates method of high order giving a quasi exact numerical solution. This clearly indicates a choice between $2 \times 2 = 4$ possibilities in obtaining the field of radiation inside a given vessel. If there is no doubt that the reference solution will be obtain using actual radiative properties with d-S_N methods, there is a need to discuss and compare the results obtained by other (approximate) methods in term of accuracy. Because this comparison does not depend on the geometry of the retained system, we will used in the following a simple Cartesian system of coordinates with a practical illumination by one side, because it is rather easiest to analyse and understand. Moreover, an order of 32 for the quadrature has been decided to be sufficiently accurate and fast for the simulation.

Figures 4 and 5 display the results obtained by simulation for the relative light flux density q/q_0 and the relative irradiance G/q_0 (diffuse incidence and typical properties of a micro-organism) for the four possibilities previously discussed.

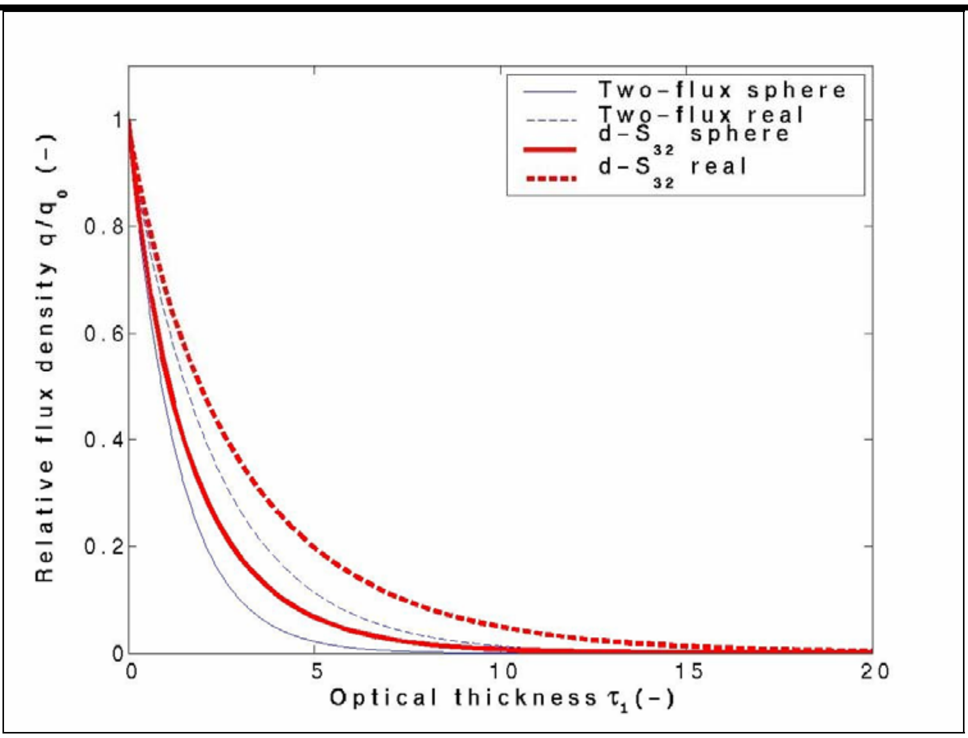

Figure 4: Comparison between different approximations in obtaining the relative profile in light flux density. The exact solution of the RTE is given using a d-S_{32} method with actual radiative properties of the micro-organism (dashed and thick line). Other simplified assumptions are compared, using either the approximate two-flux method or the approximate equivalent sphere radiative properties for micro-organisms. Calculations were performed in rectangular coordinates (illumination by one side) using the properties of *Arthrospira platensis* at 540 nm as model of particle.

Clearly, important discrepancies appear between the three approximate methods in comparison with the exact solution (true radiative properties and d-S_{32} method). Surprisingly however, at the opposite of a generally well-admitted (but not really documented) observance in the literature, two families of different behaviours are demonstrated: the two-flux method with exact radiative properties represents a quite good approximation of the exact solution (better in irradiance than in flux density), mainly for low optical thicknesses, whereas using properties of equivalent spheres leads to very important discrepancies, even using the d-S_{32} method to solve the RTE. Consequently, it can be kept in mind that the influence of radiative properties on the result is much more important than the influence of the method in solving the RTE itself. To our knowledge, this point is also demonstrated and discussed for the first time.

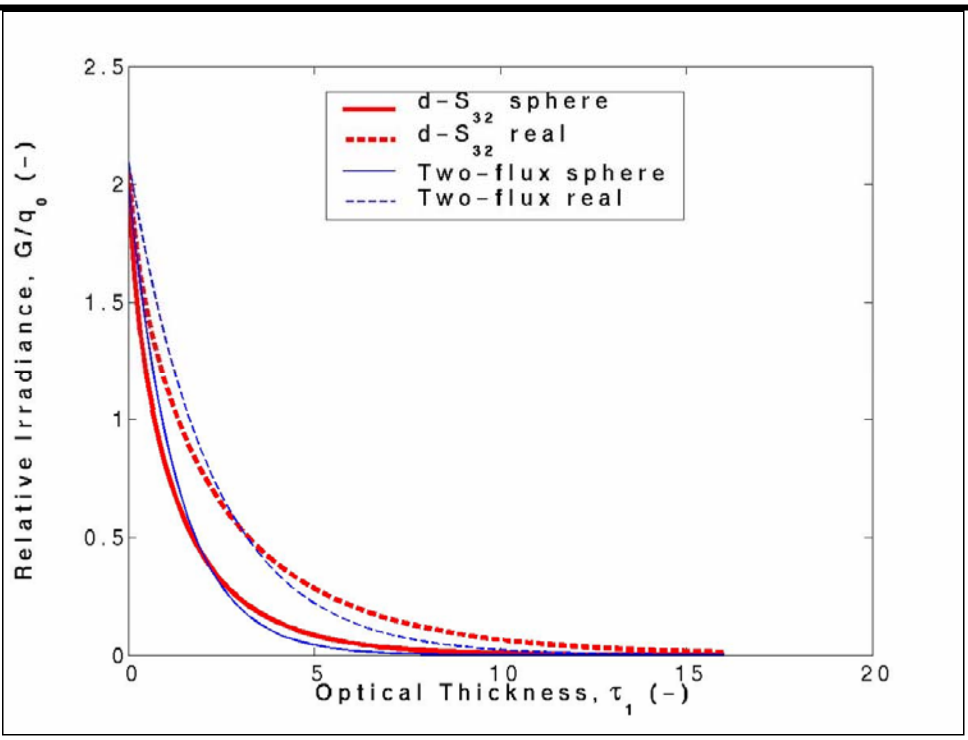

Figure 5: Comparison between different approximations in obtaining the relative profile in irradiance. The exact solution of the RTE is given using a d-S_{32} method with actual radiative properties of the micro-organism (dashed and thick line). Other simplified assumptions are compared, using either the approximate two-flux method or the approximate equivalent sphere radiative properties for micro-organisms. Calculations were performed in rectangular coordinates (illumination by one side with diffuse incidence) using the properties of *Arthrospira platensis* at 540 nm as model of particle.

4 COMPARISON BETWEEN RIGOROUS SPECTRAL APPROACH AND THE USE OF WAVELENGTH AVERAGED PARAMETERS

In the preceding developments, all the variables and parameters that we introduced were spectral values because clearly, the radiative properties of photosynthetic micro-organisms depend strongly on the wavelength in the visible domain. Nevertheless, in practice, the variables experimentally measured (flux densities, irradiances or fluence rates) are not spectral values but averaged values on a given range of wavelength (for example, the famous PAR or photosynthetically active radiation).

Consequently, if it is desired to work with rigorous spectral variables, it is necessary first to know the spectral incident light flux density in a given domain of wavelength $\Delta\lambda_i$ (from the emission spectrum of the incoming radiation) before solving the RTE N times (N corresponding to the number of discrete wavelengths for which the calculation is done with preliminary known spectral radiative properties in this domain). This more rigorous approach requires of course an important calculation time because it is necessary to calculate 300 radiative properties and then 300 profiles, if for example, the evaluation is done for each nanometre in the visible spectrum. Another possibility sketched in the first part of the TN is to use only one mean value of the radiative properties and then a direct assessment of the radiation field by solving the RTE. In this case, it is necessary to estimate the deviation obtained from the previous and exact reference situation.

We will discuss about this with the more important key variable in the PBR, necessary to formulate the coupling between the light transfer and growth kinetic rates by mean of energetic and quantum yields (Cornet *et al.,* 2001 and 2003), i.e. the local volumetric rate of radiant energy absorbed (LVREA), denoted A_λ. As appearing in the local balance of radiant light energy (eq. 70), the LVREA is linked to the irradiance by its definition:

$$A_\lambda = a_\lambda G_\lambda \qquad (74)$$

Its wavelength-averaged value will determine the growth rate of any photosynthetic micro-organism. From a mathematical point of view, this average is defined as:

$$A = \int_{\lambda_{\min}}^{\lambda_{\max}} a_\lambda G_\lambda \, d\lambda \cong \sum_{i=1}^{N} a_{i,\lambda} G_{i,\lambda} \Delta\lambda_i \qquad (75)$$

with λ_{min} and λ_{max} the limits of the wavelength range.

Of course, an exact integration implies the knowledge of analytical expressions for G_λ and a_λ, that is why the average value is generally postulated as a discrete sum.

The calculation of the LVREA by mean of eq. (75) from any given model of radiative transfer requires indeed, to know the spectral distribution of the incident radiative flux density $q_{\cap,\lambda}$. It can be calculated, knowing the incident spectrum of the lamps (Cassano *et al.*, 1995), but for a sake of convenience, it will be supposed independent of the wavelength for the considered study, giving $q_{\cap,\lambda} = q_{\cap} / N$. At the opposite, the easiest and fastest solution consists in using mean radiative properties in wavelength (considering a mean photon from the incident emission spectrum) derived from the mean optical properties as defined in part 1 of this TN, and then requiring only one calculation for all the spectrum. An intermediate way is to evaluate the mean radiative properties from the knowledge of the spectral values by the integral:

$$a, s = \frac{1}{\Delta\lambda} \int_{\lambda_{\min}}^{\lambda_{\max}} a_\lambda, s_\lambda \, d\lambda \qquad (76)$$

For these two last solutions, the mean LVREA A_m is then simply defined and calculated from the knowledge of the incident light flux density $q_{\cap}$ as:

$$A_m = aG \qquad (77)$$

One can denote that absorption coefficient and irradiance are not spectral anymore, in above equation, because they were calculated from the mean photon wavelength.

Finally, eq. (75) and (77) are two different ways in obtaining the same spectral averaged LVREA prior to the kinetic coupling formulation. They can be compared defining for convenience a dimensionless ratio by comparison with the maximum volumetric rate of radiant energy absorbed (MVREA), denoted $\langle A_0 \rangle$. This latter quantity is simply obtained, in condition of physical light limitation functioning, from the radiant incident light flux $q_{\cap}$ and the specific illuminated area of the PBR, i.e. for a one-dimensional Cartesian geometry (and neglecting the reflection at the boundaries):

$$\langle A_0 \rangle = \frac{q_{\cap}}{L} \qquad (78)$$

The profiles of relative LVREA were calculated, from a rigorous approach using wavelength bandwidth of one nanometre leading to $A/\langle A_0 \rangle$ (eq. 75), and from the mean radiative properties leading to the ratio $A_m/\langle A_0 \rangle$ (eq. 77). The results are compared on Figure 6 in case of a rectangular PBR illuminated by one side with typical micro-organisms properties, showing the discrepancies obtained when the simple approach using directly mean properties is used.

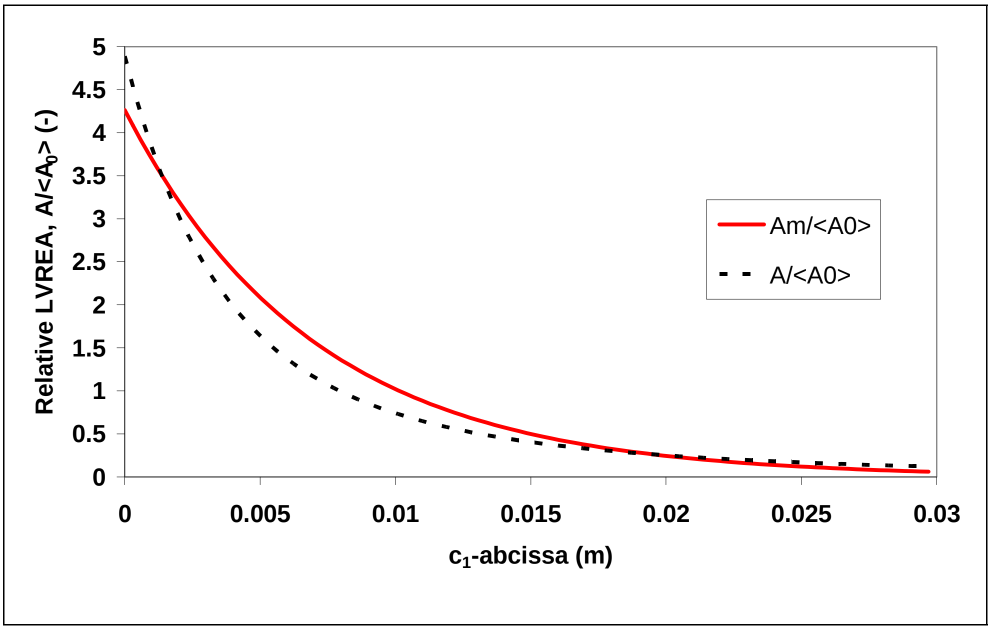

Figure 6: Comparison between the two proposed methods in averaging the dimensionless LVREA versus the c_1-abscissa in case of a rectangular vessel illuminated by one side. The dashed line corresponds to a normalized rigorous averaging of the spectral LVREA (eq. 75) giving $A/\langle A_0 \rangle$, and the continuous line corresponds to a normalized direct mean LVREA (eq. 77), $A_m/\langle A_0 \rangle$. The radiative properties used are those of *Rs. rubrum* at 1g/L.

On Figure 7, the relative difference between the two methods is quantified using the rigorous integral average as reference, leading to define the deviation as follows:

$$R.D \quad [\%] = \left(\frac{A - A_m}{A} \right) \qquad (79)$$

The obtained results show important local deviations. The more important discrepancy between the approximate and rigorous methods is observed when the light is strongly attenuated, corresponding to the green part of the visible spectrum, which is mainly scattered. In this case, the deviation may reach 60 % or more, but for low absolute irradiances. This comparison shows that rigorously, it is important to work with integral spectral LVREA if possible, because the mean LVREA approach can lead to erroneous biomass volumetric rates if a local coupling is formulated.

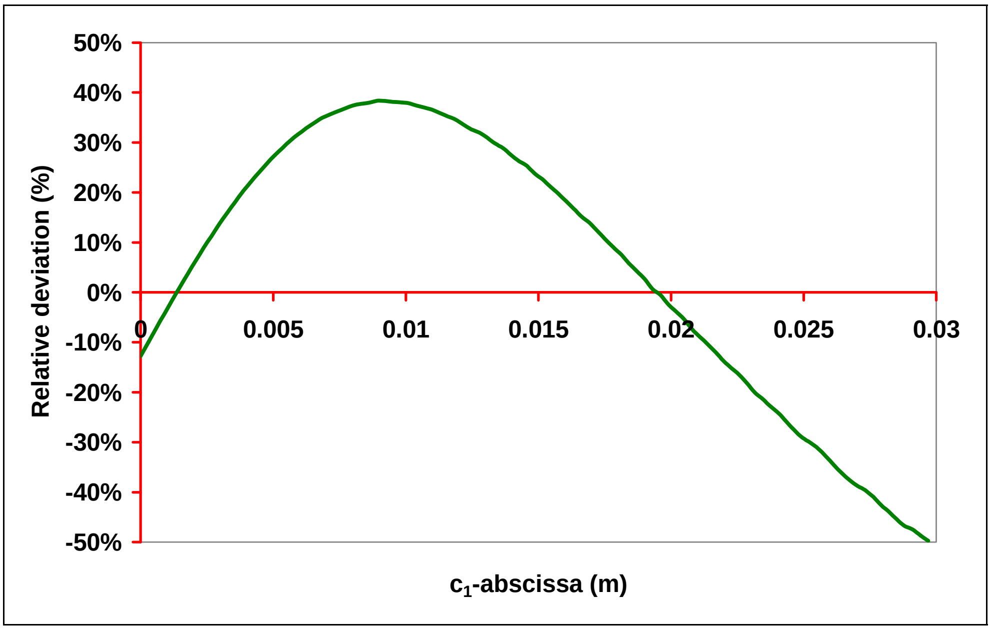

Figure 7: Relative deviation (eq. 79) between the two proposed methods in averaging the dimensionless LVREA versus the c_1-abscissa corresponding to Figure 6. The reference method retained is the more rigorous spectral averaging $A/<A_0>$.

At the opposite, if direct averaged values <A> on the PBR are calculated (for more empirical approaches of kinetic rates calculation or in case of physical limitation by light) from the photonic phase radiant energy balance (Cornet – HDR) instead of averaging irradiances of the material phase, only the reflected part of light at the incident boundary of the medium needs to be known, then the discrepancy never overcomes 10 % by this way. Special attention must be paid on the important deviations appearing for low irradiances, leading to erroneous assessment of the localisation of the compensation point for photosynthesis in the PBR and then to the definition of the working illuminated volume (Cornet *et al*., 1998).

CONCLUSIONS AND PERSPECTIVES

In this technical note, we presented and discussed theoretical developments up-grading the radiant light transfer modelling in photobioreactors of any geometries as long as the one-dimensional assumption was applicable.

Particularly, we explained a general method enabling to calculate the radiative properties involved in the radiative transfer equation (absorption and scattering coefficients with the phase function), only from the preliminary knowledge of optical properties of given micro-organisms, requiring only basic information such as their shape, their size distribution and their pigment content. Different methods were then envisaged to solve the RTE, examining both analytical approximated generalised two-flux methods and full numerical methods of different orders, the highest leading to an exact reference solution. Finally, these results were used to discussed the validity in using mean coefficients in place of rigorous averaging of each spectral coefficient in the determination of fields of irradiances or local volumetric rates of radiant energy absorbed (LVREA). These quantities are of prior importance in formulating the kinetic or stoichiometric coupling (by a predictive thermodynamics approach) in the framework of the royal route toward PBR modelling proposed in LGCB.

As a result, the calculation of the radiation field inside a PBR is now became a completely predictive problem, both in rectangular or curvilinear systems of coordinates. This means that, if the basic characteristics of a micro-organism are known, it is possible, from the knowledge of the boundary conditions, to accede to the irradiance or the LVREA fields inside the reactor *a priori*, without any other experimental parameter or determination. This is a crucial point for future scale-up of PBR, high-size PBR simulation and/or control, or developing new design of PBR with high productivities. The new rigorous developments presented in this TN (mainly in cylindrical coordinates) have also led to revisit the calibration method used in the MELiSSA group for the determination of the mean radiant incident light flux density from the spherical photon fluence rate sensor put at the centre of the reactor. The new treatment is presented and debated in the appendix 1 of this TN and will serve hereafter as a reference method.

Clearly, the level of sophistication reached in this TN for the radiative transfer modelling is an achievement result (giving exact solutions) and should not be modified in the future as soon as one-dimensional approximation are concerned. For more complicated, three-dimensional situations, it is possible to use a finite element method (FEM) using the characteristic curve algorithm, previously developed in the lab, but it then requires further developments in order to include in the method the **P**-matrix giving the exact phase function for scattering.

Finally, the validity of all the theoretical tools presented in this document will be discussed in the next TN 83.3 dealing with experimental measurements in a high accuracy optical bench with an integrating sphere photometer, considering both *Rs. rubrum* and *A. platensis* as the more important photosynthetic micro-organisms in the MELiSSA team.

Notations

Roman Letters

a_λ , a	Volumetric absorption coefficient (spectral or mean) [m^{-1}]
a	Minor semi-axis of the particle (radius for a sphere) [m]
a_n	Lorenz-Mie coefficient [0]
A	Local volumetric rate of radiant energy absorbed [W.m^{-3}]
$A(\Theta,\Phi)$	Integral amplitude function for the AD approximation [0]
A_m	Mean (spectral) local volumetric rate of radiant energy absorbed [W.m^{-3}]
$A_R = b/a$	Asphericity ratio [0]
$<A_0>$	Maximum means volumetric rate of radiant energy absorbed [W.m^{-3}]
b	Major semi-axis of the particle (defining the rotation symmetry axis) [m]
$\overline{b}$	Backward scattered fraction [0]
b_n	Lorenz-Mie Coefficient [0]
c_1	First coordinate in the mobile frame of reference [m]
c_2	Second coordinate in the mobile frame of reference [m]
c_3	Third coordinate in the mobile frame of reference [m]
C	Cross section of the particle [m^2]
C_X	Biomass concentration [kg.m^{-3}]
d_p	Particle diameter [m]
D	Cylinder diameter [m]
$\mathbf{D}_\mathrm{N}$	The N*N eye matrix [0]
e_λ, e	Volumetric extinction coefficient (spectral or mean) [m^{-1}]
$\mathbf{E}$	Electric field [V.m^{-1}]
Ea_λ, Ea	Mass absorption coefficient (spectral or mean) [m^2.kg^{-1}]
Ei (n,x)	Integral exponential function [0]
Es_λ, Es	Mass scattering coefficient (spectral or mean) [m^2.kg^{-1}]
f	Intra-particle volume fraction [0]
f_v	Particle volume fraction [0]
F	Mueller matrices coefficient [0]
G_a	Cross sectional area for the particle [m^2]
G_λ	Spectral irradiance [W.m^{-2}.m^{-1}]
G	Irradiance [W.m^{-2}]
$h_n^{(2)}(x)$	Spherical Hankel function [0]
$\mathbf{H}$	Magnetic field [A.m^{-1}]
$I_n(x)$	Modified first kind Bessel function of order n [0]
I_λ	Specific intensity [W.m^{-2}.sr^{-1}.m^{-1}]
I_λ^+	Positive hemispheric intensity [W.m^{-2}.sr^{-1}.m^{-1}]
I_λ^-	Negative hemispheric intensity [W.m^{-2}.sr^{-1}.m^{-1}]
$I_{\lambda,\cap}$	Incident specific intensity [W.m^{-2}.sr^{-1}.m^{-1}]
$j_n(x)$	Spherical Bessel function of first kind [0]

k_h	Angular radiation hypothesis factor [0]
k	Wave number [m^{-1}]
L	Length of the vessel (rectangular system) [m]
$\mathbf{M}$	Diagonal μ-matrix [0]
m	Number of angular coordinates in a geometry [0]
m_λ, m	Complex refractive index (spectral or mean) [0]
n_λ, n	Real part of the refractive index (spectral or mean) [0]
$n(r, x)$	Size distribution law [0]
n_p	Number of points per profile [0]
N	Quadrature order or number of wavelength [0]
N_p	Volume density of particles [m^{-3}]
$p_\lambda(\Theta), p(\Theta)$	Phase function for scattering (spectral or mean) [0]
$\mathbf{P}$	Matrix describing the phase function for scattering [0]
$\mathbf{P}$	Poynting vector [$W.m^{-2}$]
$P_n^m(x)$	Legendre polynomial [0]
$\mathbf{q}_\lambda$	Spectral light flux density vector [$W.m^{-2}.m^{-1}$]
$q_{\lambda,\cap}$	Incident spectral light flux density [$W.m^{-2}.m^{-1}$]
q	Light flux density [$W.m^{-2}$]
$q_\cap, q_0$	Incident light flux density [$W.m^{-2}$]
Q	Particle efficiency [0]
$Q^\bullet$	Mean correction factor [0]
$Q_\lambda^\bullet$	Spectral correction factor [0]
r	Radius [m]
r_{32}	Sauter effective radius [m]
r_b	Radius of the spherical photon fluence rate sensor [m]
r_s	Radius of the enlightening sphere [m]
R	Radius of the PBR [m]
s_λ, s	Volumetric scattering coefficient (spectral or mean) [m^{-1}]
$\mathbf{S}$	Amplitude scattering Matrix (spherical coordinates) [0]
S_i	Amplitude function (spherical coordinates) [0]
V_p	Volume of the particle [m^3]
w	Weight of the quadrature [0]
w_i	Quadrature coefficient [0]
w_j	Mass fraction for species j [0]
$\mathbf{W}$	Diagonal w-matrix [0]
W_λ	Spectral energy distribution for the light emission device [0]
x	First coordinate in rectangular system [m]
x, x_a	Size parameter $= 2 \pi a n_m / \lambda$ [0]
x_w	Water volume fraction [0]
y	Second coordinate in rectangular system [m]
$y_n(x)$	Bessel spherical function of second kind [0]
z	Length [m]

z	Third coordinate in rectangular system [m]

Greek Letters

α_λ	Linear scattering modulus [0]
β	Zenith of the unitary direction vector $\mathbf{\Omega}$ [rad]
γ	Angle [rad]
δ_λ	Extinction coefficient for the generalised two-flux method [m^{-1}]
$\delta_{X=X_0}$	Krönecker delta centred on $X=X_0$ [0]
ε_r	Relative permittivity or dielectric constant [0]
ε_λ	Spectral permittivity [$F.m^{-1}$]
$\zeta_n(x)$	Riccati-Bessel function [0]
θ	Polar angle (incident) [rad]
θ_r	Zenith of the position vector [rad]
Θ	Scattering polar angle ($\theta - \theta'$) [rad]
$\kappa^\bullet$	Imaginary part of the mean refractive index [0]
κ_r	Relative imaginary part of the refractive index [0]
κ_λ, κ	Imaginary part of the refractive index (spectral or mean) [0]
λ	Wavelength [m]
μ	Cosine of β angle [0]
ξ	Azimuth of the unitary direction vector $\mathbf{\Omega}$ [rad]
$\pi_n(\theta)$	Derivative function of the Legendre polynomial [0]
ρ, ρ_λ	Spectral phase shift of the wave [0]
ρ_a	Real part of the phase shift of the wave [0]
ρ_j	Density of species j [$kg.m^{-3}$]
τ	Reduced coordinate [0]
$\tau_n(\theta)$	Derivative function of the Legendre polynomial [0]
ϕ_r	Azimuth of the position vector [rad]
Φ	Scattering azimuthal angle ($\phi - \phi'$) [rad]
ψ	Photon fluence rate [$\mu E.m^{-2}.s^{-1}$ = μmol of photons. $m^{-2}.s^{-1}$]
$\psi_n(x)$	Riccati-Bessel function [0]
ω	Albedo number [0]
Ω	Solid angle [sr]
$\mathbf{\Omega}$	Unitary direction vector [0]
$\mathbf{\Omega}_P$	Projection of the unitary direction vector on plane (c_2 ; c_3) [0]

Subscripts

0	Relative to the particular $r = 0$ value (centre) in cylindrical reactor [-]

a	Relative to radius or semi-axe of the particle [-]
ABS	Relative to absorption [-]
c	Collimated [-]
cm	Relative to cell material [-]
cyl	Relative to a plan perpendicular to the major axis of a cylinder [-]
d	Diffuse [-]
dry	Relative to dry biomass [-]
eff	Effective parameter (taking into account the size distribution) [-]
eq	Equivalent quantity (in volume) [-]
EXT	Relative to extinction [-]
m	Relative to surrounding medium or minimum [-]
M	Maximum [-]
p	Particle [-]
pig	Relative to photosynthetic pigments [-]
PHB	Relative to polyhydroxybutyrate content [-]
r	Optical quantity relative to surrounding medium [-]
R	Relative to the radius of the reactor considered as boundary [-]
SCA	Relative to scattering [-]
θ	Relative to incident polar direction θ [-]
λ	Relative to the wavelength λ [-]
$//$	Parallel polarisation [-]
$\perp$	Perpendicular polarisation [-]

Superscripts

$*$	Relative to a complex conjugate [-]
$'$	Real part of a complex number [-]
$''$	Imaginary part of a complex number [-]

Others

$\mathrm{Re}\{\ \}$	Real part [-]
$\mathrm{Im}\{\ \}$	Imaginary part [-]
$\hat{u}$	Complex variable associated with u [-]
$\bar{u}$	Mean quantity (over all the incident directions θ for randomly oriented particles) [-]

Abbreviations

AD	Anomalous diffraction
PHB	Polyhydroxybutyrate

PBR	Photobioreactor
RTE	Radiative transfer equation
TE	Transverse electric
TM	Transverse magnetic

References

AIBA S. 1982. Growth kinetics of photosynthetic micro-organisms. *Adv. Biochem. Eng.*, **23**: 85-156.

ASANO S., SATO M. 1980. Light scattering by randomly oriented spheroidal particles. *Appl. Optics*. **19:** 962-974.

BIDIGARE R. R., ONDRUSEK M. E., MORROW J. H., KIEFER D. A. 1990. *In vivo* absorption properties of algal pigments. *SPIE Ocean Optics X*. **1302:** 290-302.

BOHREN C. F., HUFFMAN D. R. 1983. *Absorption and Scattering of Light by Small Particles*. John Wiley and Sons, New York.

CASSANO A. E., MARTIN C. A., BRANDI R. J., ALFANO O. M. 1995. Photoreactor analysis and design: fundamentals and applications. *Ind. Eng. Chem. Res*. **34**: 2155-2201.

CHANDRASEKHAR S. 1960. *Radiative Transfer*. Dover, New York.

CORNET J-F. *Procédés limités par le transfert de rayonnement en milieu hétérogène – Étude des couplages cinétique et énergétique dans les photobioréacteurs par une approche thermodynamique*. Habilitation à Diriger les Recherches, Université Blaise Pascal, Clermont-Ferrand, France (to be appeared in 2007).

CORNET J-F., DUSSAP C-G., DUBERTRET G. 1992. A structured model for simulation of cultures of the cyanobacterium *Spirulina platensis* in photobioreactors: Coupling between light transfer and growth kinetics. *Biotech. bioeng*., **40**: 817-825.

CORNET J-F., DUSSAP C-G., GROS J-B. 1998. Kinetics and energetics of photosynthetic micro-organisms in photobioreactors. *Advances in biochemical engineering/Biotechnology*: **59**, 153-224.

CORNET J-F., DUSSAP C-G., GROS J-B., BINOIS C., LASSEUR C. 1995. A simplified monodimensional approach for modeling coupling between radiant light transfer and growth kinetics in photobioreactors. *Chem. Eng. Sci.*, **50:** 1489-1500.

CORNET J-F., DUSSAP C. G., LECLERCQ J-J. 2001. Simulation, design and model based predictive control of photobioreactors. In: Hofman M. and Thonart P. eds., *Focus on biotechnology 4: Engineering and manufacturing for biotechnology*. Kluwer Academic, Dordrecht, pp. 227-238.

CORNET J-F., FAVIER L., DUSSAP C. G. 2003. Modelling stability of photoheterotrophic continuous cultures in photobioreactors. *Biotechnol. Prog*. **19:** 1216-1227.

CORNET J-F., FAVIER-TEODORESCU L., DUSSAP C. G. 2005. Modelling of *Rhodospirillum rubrum* growth in cylindrical photobioreactor – Stability analysis of continuous cultures and operating domain definition. Technical Note 55.1. ESA contract MOU TOS-MCT/2002/316/In/CL.012.

DAVIS P., RABINOWITZ P. 1956. Abscissas and weights for Gaussian quadratures of high order. *Journal of research of the National Bureau of Standards*. **56:** 35-37.

HEASLET M.A., WARMING R.F. 1966. Theoretical predictions of radiative transfer in a homogeneous cylindrical medium. *J. Quant. Spectrosc. Radiat. Transfer*. **6**: 751-774.

KUMAR S., MAJUMDAR A., TIEN C.L. 1990. The differential-discrete ordinate method for solutions of the equation of radiative transfer. *Journal of heat transfer*. **112**: 424-429.

MENGÜC M. P., VISKANTA R. 1983. Comparison of radiative transfer approximations for a highly forward scattering planar medium. *J. Quant. Spectrosc. Radiat. Transfer*. **29:** 381-394.

MICHELS H. H. 1963. Abcissas and weight coefficient for Lobatto quadrature. *Mathematics of computation*. **17**: 237-244.

MISHCHENKO M. I., HOVENIER J. W., TRAVIS L. A. (EDS). 2000. *Light scattering by nonspherical particles: theory, measurements and applications.* Academic Press.

MISHCHENKO M. I., TRAVIS L. D. 1998. Capabilities and limitations of a current Fortran implementation of the T-Matrix method for randomly oriented, rotationally symmetric scatterers. *J. Quant. Spectrosc. Radiat. Transfer*. **60:** 309-324.

POTTIER L., PRUVOST J., DEREMETZ J., CORNET J-F., LEGRAND J., DUSSAP C. G. 2005. A fully predictive model for one-dimensional light attenuation by *Chlamydomonas reinhardtii* in a torus photobioreactor. *Biotechnol. Bioeng*. **91:** 569-582.

RAMKRISHNA D., AMUNDSON N.R. 2004. Mathematics in Chemical Engineering: A 50 Year introspection. *AIChE Journal*. **50:** 7-23.

SIEGEL R., HOWELL J. R. 2002. *Thermal radiation heat transfer.* Taylor and Francis, New York, 4th ed.

THYNELL S. T. 1989. The integral form of the equation of transfer in finite, two-dimensional, cylindrical media. *J. Quant. Spectrosc. Radiat. Transfer*. **42**: 117-136.

VAN DE HULST H. C. 1981. *Light scattering by small particles*. Dover Publications Inc., New York, 2nd ed.

VAN NOORT M., HUBENY I., LANZ T. 2002. Multidimensional non-LTE radiative transfer. I. A universal two-dimensional short-characteristics scheme for cartesian, spherical, and cylindrical coordinate systems. *The Astrophysical journal*. **568**: 1066-1094.

WYATT P. J. 1968. Differential light scattering: a physical method for identifying living bacterial cells. *Appl. Optics*. **10:** 1879-1896.

WYATT P. J. 1972. Light scattering in the microbial world. *J. Coll. Interf. Sci*. **39:** 479-491.

APPENDICES

APPENDIX 1
Revisiting the incident hemispherical light flux density ($q_\cap$) calibration method with new cylindrical models

Since the early stage of radiative model developments in the MELiSSA group, a special attention has always been paid to the experimental determination of the hemispherical incident light flux density $q_\cap$ sometimes referred as just the "incident light flux" onto the PBR (q_0 or q_R). This variable is really of crucial importance because it completely defines (with the geometry) the local radiative transfer inside the PBR, and then both the actual (kinetics mode) and physically light-limited functioning (maximum performances) of a given PBR. Generally speaking, for a complicated geometry, this variable is not directly available and the boundary conditions must be obtained in specific intensity for each considered incident direction, discretising the hemispherical solid angle from a model of emission for the lamps. In many cases however, the geometry of the problem is such as it is possible to use the one-dimensional approximation for the rectangular or cylindrical radiative transfer problems (as depicted in this TN). It is then possible to just use the incident light flux density $q_\cap$ in completely defining the boundary conditions onto the reactor. In the last decade, three ways have been used in the MELiSSA team in order to assess the value of this incident flux with the best accuracy as possible:

- a calculation from the energetic yield of the lamps versus the electric power and the geometry of the reactor;
- an experimental method in any geometry of reactor using a chemical actinometer (the Reinecke salt);
- only for cylindrical PBR, a calculation form the measurement of a spherical sensor (usually named E_b) put at the centre of the reactor.

If the two first methods are always available, the latter is likely the more convenient and practical in case of cylindrical geometries, and it was the more often used in the different lab of the group. Unfortunately, it is today necessary to revise this method for at least four reasons that we will try to explain in the following.

- The first point is that we considered only a particular angular distribution for the radiation field at the boundaries and inside the PBR for one-dimensional applications (e.g. a diffuse isotropic field in case of Schuster assumptions), whereas it is necessary to distinguish at least two different cases with eventually intermediate hypotheses for the incident light flux density (see this TN).

- The second point is that the spherical sensor used does not measure an averaged area irradiance E_b as we thought for a long time, but it really measures a photon fluence rate ψ (the definition of which being quite different).

- The third point is that the theoretical relation used in the past to calculate the incident flux $q_{\cap}$ from the sensor measure E_b, was established in seeking the limit in very dilute conditions of an averaged area relation using the previous model expression for the radius profile irradiance G_r (eq. 5 of TN 55.1). Moreover, we have already discussed in TN 55.1 that this approximated relation was not available in case of dilute medium or if the radius was kept equal to 0, which are exactly the two necessary conditions for our present purpose!

- Finally, the last point is that until now, we always used in our calculation an incident spectrum corresponding to the absorbed radiation in the PBR, i.e. a range between 350 and 750 nm for *Spirulina*. This range is wider than the usual retained range (the famous PAR for photosynthetically active radiation in the range 400-700 nm) when it is desired to work with moles of photon per second instead of watts for the definition of the radiant power available by photosynthesis. Today, because the new knowledge models for coupling radiant light transfer and rates developed in LGCB use rather a quantum yield approach (applying the linear irreversible processes thermodynamics relationships for its calculation), it seems necessary to work with incident light fluxes or irradiances defined in the PAR, taking then into account only the visible wavelengths available by photosynthesis.

The first consequence of the latter point is that we propose to work in the future with incident fluxes $q_{\cap}$ and irradiances G (previously called $4\pi J$ or I_{Σ}, but the letter G is now quasi normalised in the physicist community – see TN 55.1 -) defined in the PAR for all the practical and modelling applications involving photoreactors in the MELiSSA group. The considered ranges of wavelength should then be respectively:

[400-700 nm] for *Arthrospira* (*Spirulina*) *platensis*;
[400-900 nm] for *Rhodospirillum rubrum*.

It must be noticed here that the classical range for photosynthesis (the PAR 400-700 nm) is directly the range used by commercial sensor working as quantum-meter (in µmoles of photons per square meter and per second) and then, no correction factor will be necessary in this case. In fact, for future knowledge and predictive models developed currently in the lab in formulating the kinetic and stoichiometric coupling, the use of µmoles of photons per second unit is the more convenient and general choice (mainly if it is desired to work with non-white lightening sources). Nevertheless, the energetic analysis of the PBR, with also the use of thermodynamic state functions involved in the coupling formulation, requires to use watts as the sole SI unit for power. For this reason, it is often necessary to convert one unit in the other with the highest accuracy as possible, depending on the considered wavelength spectrum as explained at the end of this appendix.

The second consequence is that we need to develop a new and rigorous relationship in calculating the incident light flux $q_{\cap}$ from the actual measurement of the photon fluence rate ψ at the centre of a cylindrical PBR using a quantum sensor (usually, the 3 cm radius r_b LI COR spherical sensor of LGCB was used for this purpose). This requires first to have a rigorous integral definition of the photon fluence rate ψ measured by any spherical quantum sensor of radius r_b. This definition is practically given as a normalised ratio to the incident irradiance G_R at the boundary of a PBR of total radius R by the following surface integral of a scalar product (see Pottier *et al.*, 2005 and Cornet – HDR):

$$\frac{\psi}{G_R} = \frac{1}{\pi r_b^2 G_R} \oiint_S \mathbf{q}_\cap \cdot d\mathbf{S} \qquad \text{(A1)}$$

Using the one-dimensional approach (corresponding to the sought incident light flux) and the rigorous two-flux cylindrical solutions developed in this TN (eq. 62b and 63), it is possible to explain the integrand and to calculate analytically the double integral (A1). Nevertheless, the general problem is far to be trivial and leads to an integration in three parts with a very complicated resulting expression. Fortunately, we are just seeking a particular and useful solution positioning the sensor at the centre of the reactor ($r = 0$, leading to ψ_0). In this case, for a very dilute culture broth (low biomass concentration), taking the limit for small values of the extinction coefficient δ, leads to the following simple expression of the integral (A1):

$$\lim_{\delta_c \to 0} \left[\frac{\psi_0}{G_R} \right] = 4\Lambda \left[1 + \frac{\alpha\,\delta_c}{4\Lambda}(r_b - 2R) \right] \qquad \text{(A2)}$$

in which the extinction coefficient is always considered for a collimated radiation $\delta_c = \sqrt{a\,(a + 2\,\bar{b}\,s)}$ and Λ being a constant factor responsible for the angular nature of the radiation field (collimated or isotropic). In the practical case where there is no culture broth between the sensor and the illuminated wall of the PBR (air or pure water only), $\delta_c = 0$ and eq. (A2) reduces simply to:

$$\frac{\psi_0}{G_R} = 4\Lambda \qquad \text{(A3)}$$

giving the relation between the photon fluence rate at the centre of the empty reactor ψ_0 and the incident irradiance at the illuminated external wall G_R. Keeping in mind that we expected a relation for the incident light flux density $q_\cap$, it is then necessary to introduce the values of Λ and G_R in the two extreme cases for the angular nature of the radiation field inside the PBR. In case of a diffuse (isotropic) radiation, Λ = ½ and $G_R = 2\,q_\cap$, but in case of a collimated radiation, $\Lambda = 1$ and $G_R = q_\cap$, showing that the final result does not depend on the nature of the radiation field, giving in all cases:

$$\boxed{\psi_0 = 4 q_\cap} \qquad \text{(A4)}$$

Surprisingly, this useful relation appears very simple and independent of the respective radii for the sensor r_b and for the reactor R (at the contrary of the preceding expression used in the MELiSSA team established 10 years ago with an approximate treatment of the RTE in cylindrical coordinates). In the future, eq. (A4) should be used to treat easily the measurements obtained with a spherical fluence rate quantum sensor in cylindrical PBR. It just shows that the

photon fluence rate at the centre of the PBR ψ_0 is four times the incident light flux density $q_\cap$ (as long as the one-dimensional assumption remains valid), and this is true whatever the angular nature of the radiation field. At the opposite, it is obviously impossible to obtain any information on this angular boundary distribution with this kind of measurement!
In the future, it will be now possible to re-process the results obtained in the past with the good formula, leading probably to different values for the incident light flux (depending of the actual ratio r_b/R of each PBR). Be sure that the authors of this TN apologise for this inconvenience, the previous erroneous treatment of this problem proceeding mainly in an underestimation of the mathematical difficulty in dealing with the RTE in curvilinear coordinates.

Finally, the conversion unit of $q_\cap$ between µmol.m^{-2}.s^{-1} and W.m^{-2} (J.m^{-2}s^{-1}), i.e. between joule and micro-Einstein, requires knowing the emission spectrum of the source, enabling to calculate the mean wavelength λ_{mean} of the photons involved in the calculation. This mean wavelength is given by the following integral from the spectral energy distribution W_λ of the source:

$$\lambda_{mean} = \frac{\int_{\lambda_{\min}}^{\lambda_{\max}} (\lambda W_\lambda) d\lambda}{\int_{\lambda_{\min}}^{\lambda_{\max}} W_\lambda d\lambda} \qquad \text{(A5)}$$

The required conversion factor between joules and µmoles of photons (or µE) is then obtained applying:

$$\boxed{1\,\mathrm{J} = \frac{\lambda_{mean}}{1.1974 \times 10^{-7}}\,\mu\mathrm{E}} \qquad \text{(A6)}$$

giving for example, with λ_{min} = 400 nm and λ_{max} = 700 nm for a typical homogeneous white emission spectrum the well-known result (λ_{mean} = 550 nm): 1 J = 4.6 µE.

APPENDIX 2
Plots for two-flux method's solutions

Rectangular System

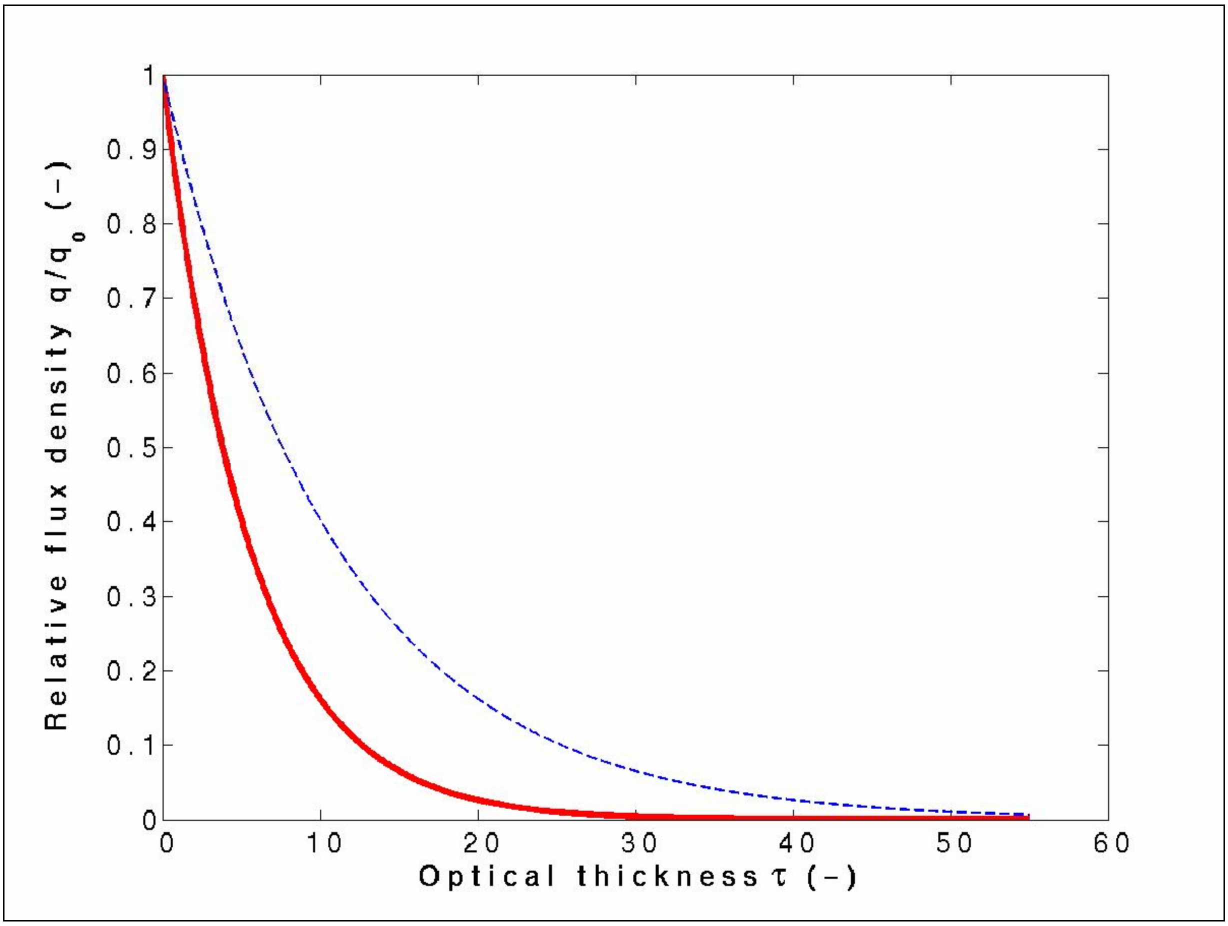

Figure A2-1: Relative light flux density in a rectangular system illuminated by one side (with negligible reflection at the rear) versus the optical thickness of the medium. Red (thick) curve corresponds to diffuse hypothesis, blue (dashed) curve corresponds to collimated hypothesis. The radiative properties of the particle used for the calculation (corresponding to a typical micro-organism) are $\omega = 0.91$ and $\bar{b} = 10^{-4}$

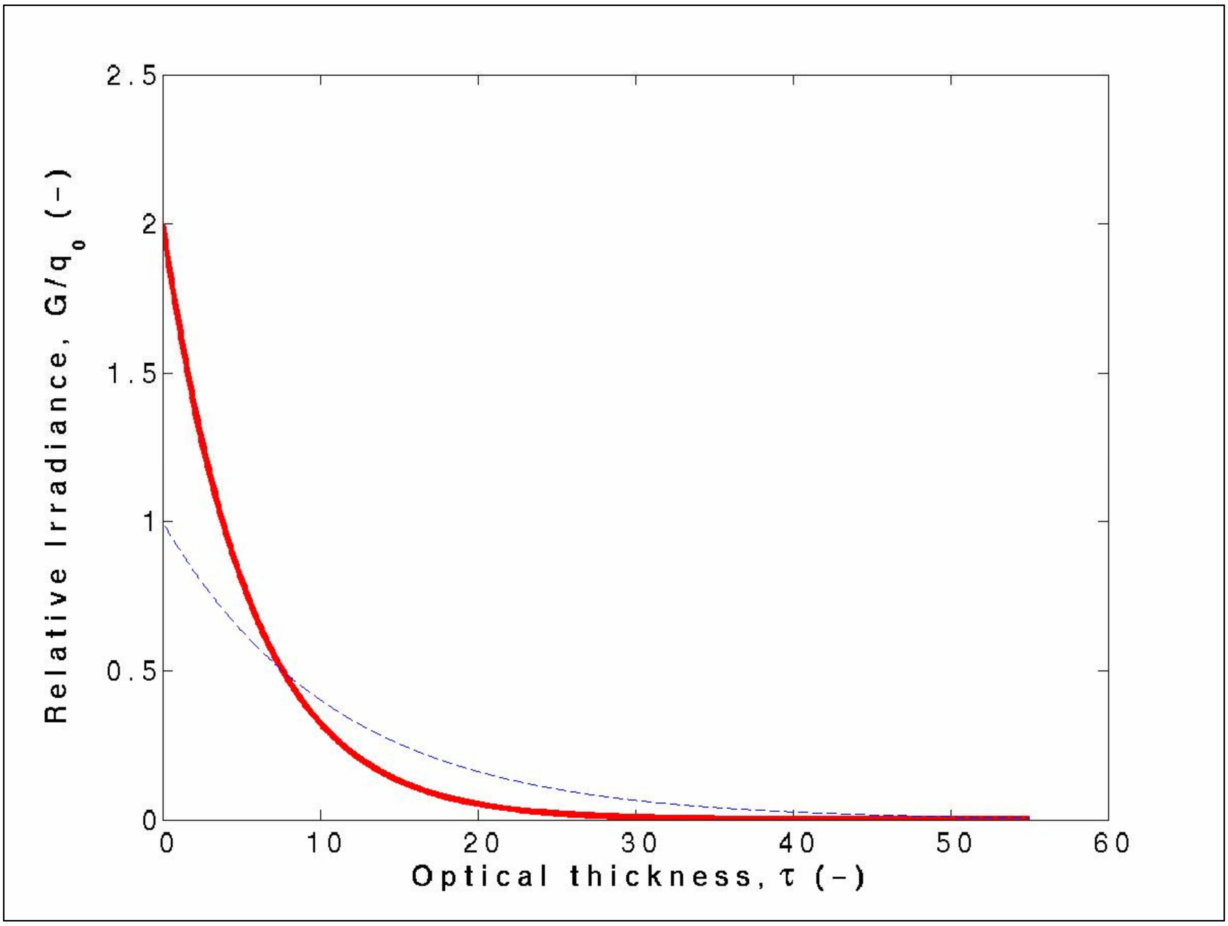

Figure A2-2: Relative light irradiance in a rectangular system illuminated by one side (with negligible reflection at the rear) versus the optical thickness of the medium. Red (thick) curve corresponds to diffuse hypothesis, blue (dashed) curve corresponds to collimated hypothesis. The radiative properties of the particle used for the calculation (corresponding to a typical micro-organism) are $\omega = 0.91$ and $\bar{b} = 10^{-4}$

Cylindrical System

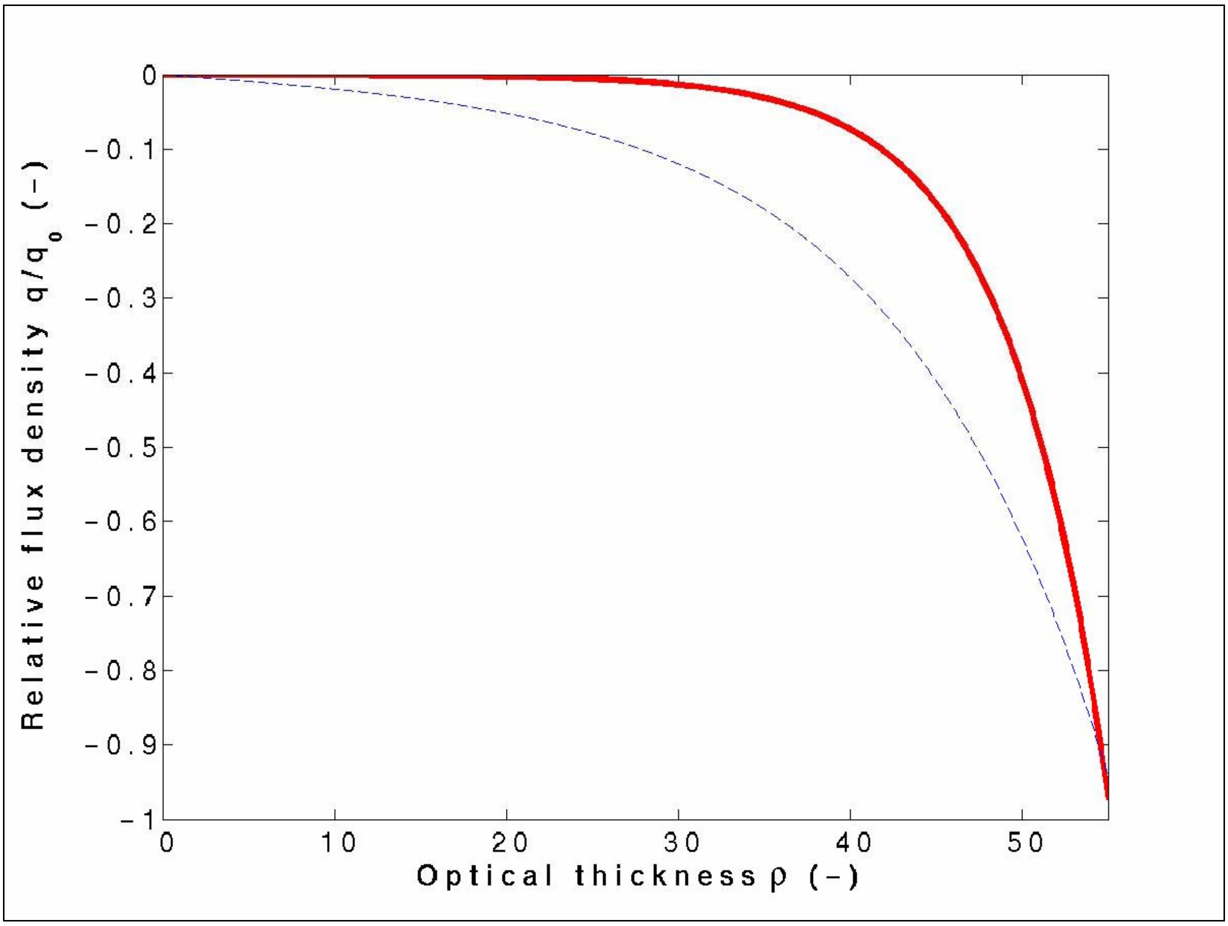

Figure A2-3: Relative light flux density in a cylindrical system radially illuminated versus the optical thickness of the medium. Red (thick) curve corresponds to diffuse hypothesis, blue (dashed) curve corresponds to collimated hypothesis. The radiative properties of the particle used for the calculation (corresponding to a typical micro-organism) are $\omega = 0.91$ and $\bar{b} = 10^{-4}$

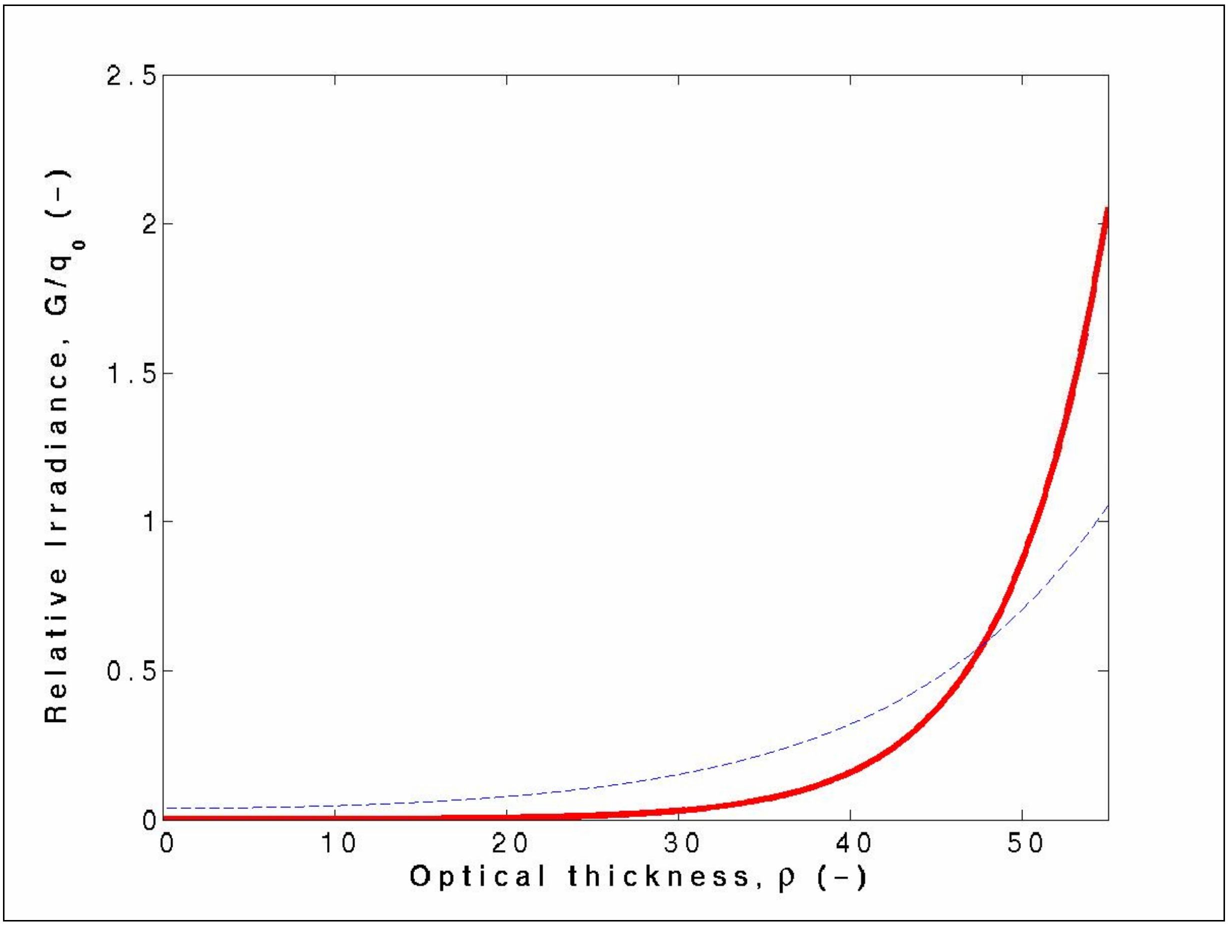

Figure A2-4: Relative light irradiance in a cylindrical system radially illuminated versus the optical thickness of the medium. Red (thick) curve corresponds to diffuse hypothesis, blue (dashed) curve corresponds to collimated hypothesis. The radiative properties of the particle used for the calculation (corresponding to a typical micro-organism) are $\omega = 0.91$ and $\bar{b} = 10^{-4}$

APPENDIX 3
Plots of d-S$_n$ method's solutions

Rectangular System

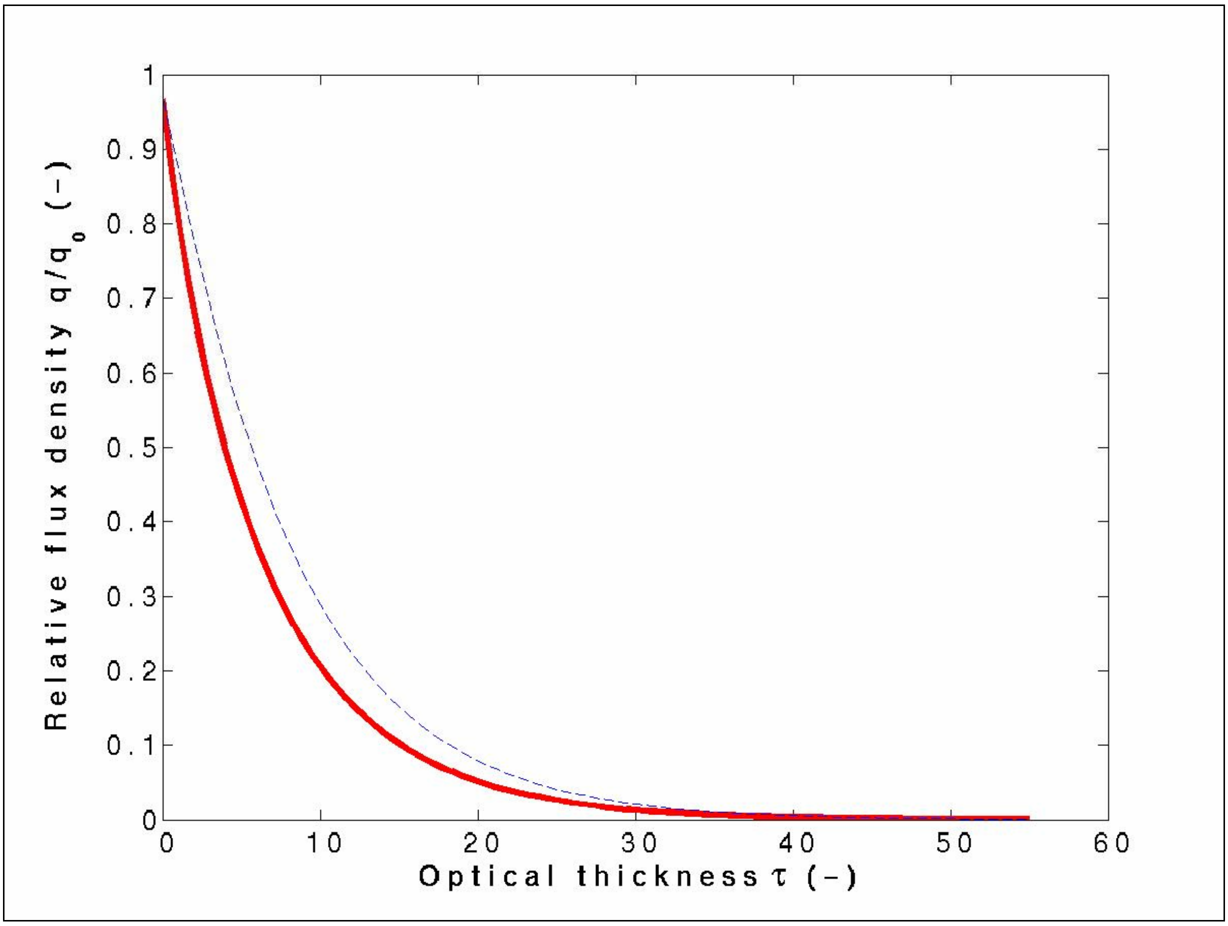

Figure A3-1 Relative light flux density in a rectangular system illuminated by one side (with negligible reflection at the rear) versus the optical thickness of the medium. Red (thick) curve corresponds to diffuse hypothesis, blue (dashed) curve corresponds to collimated hypothesis. The radiative properties of the particle used for the calculation correspond to a typical micro-organism ($\omega = 0.91$) and are the same as in Appendix 2.

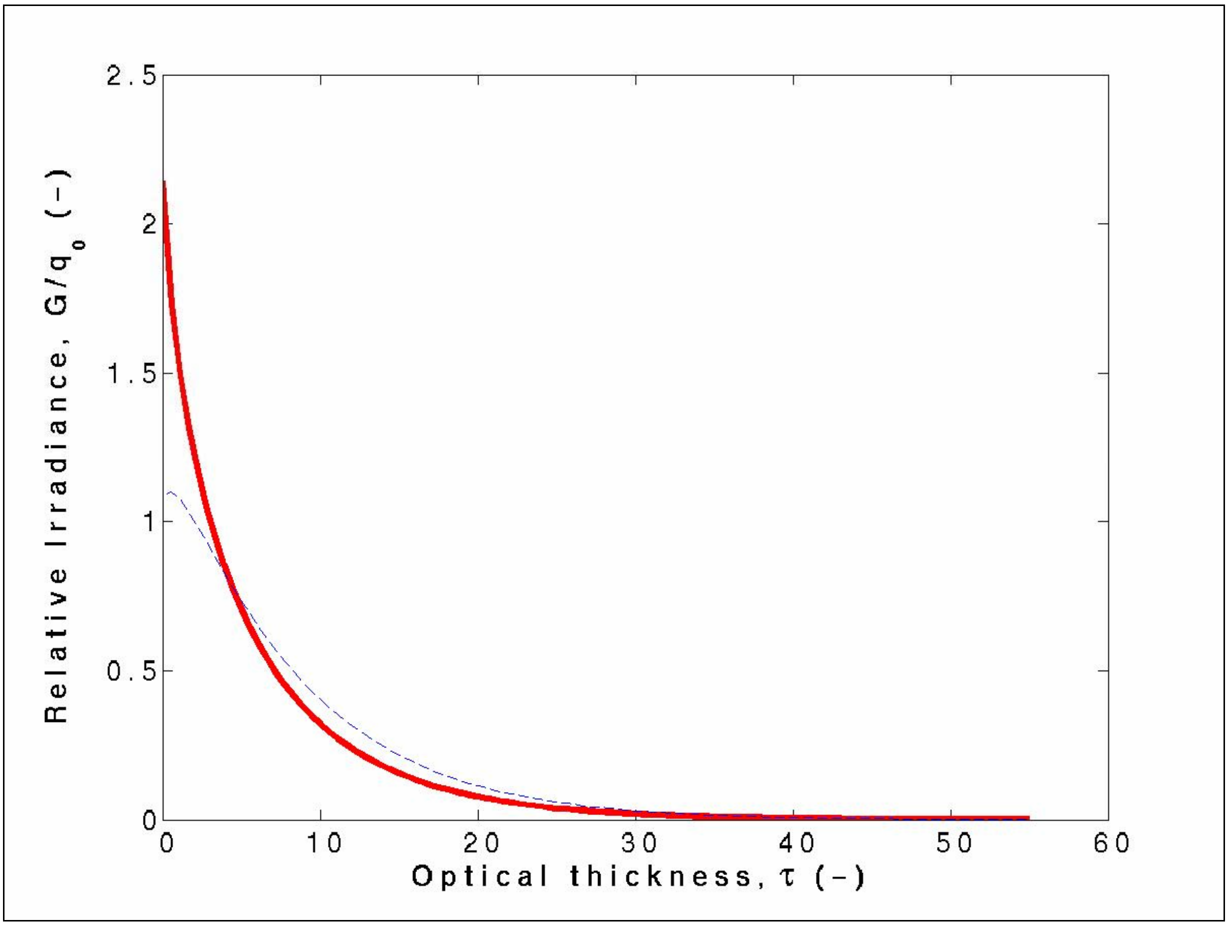

Figure A3-2: Relative light irradiance in a rectangular system illuminated by one side (with negligible reflection at the rear) versus the optical thickness of the medium. Red (thick) curve corresponds to diffuse hypothesis, blue (dashed) curve corresponds to collimated hypothesis. The radiative properties of the particle used for the calculation correspond to a typical micro-organism (ω = 0.91) and are the same as in Appendix 2.

Cylindrical System

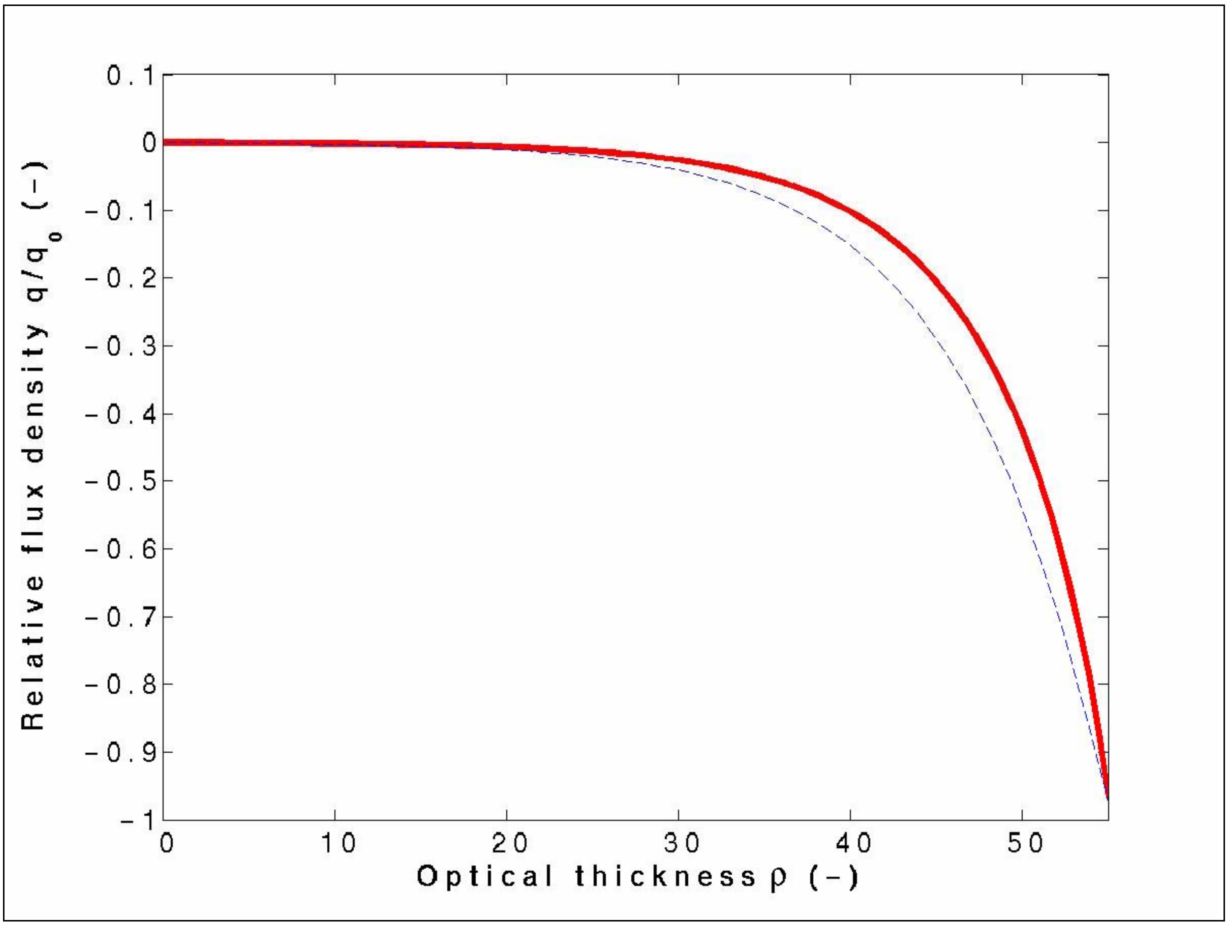

Figure A3-3: Relative light flux density in a cylindrical system radially illuminated versus the optical thickness of the medium. Red (thick) curve corresponds to diffuse hypothesis, blue (dashed) curve corresponds to collimated hypothesis. The radiative properties of the particle used for the calculation correspond to a typical micro-organism (ω = 0.91) and are the same as in Appendix 2.

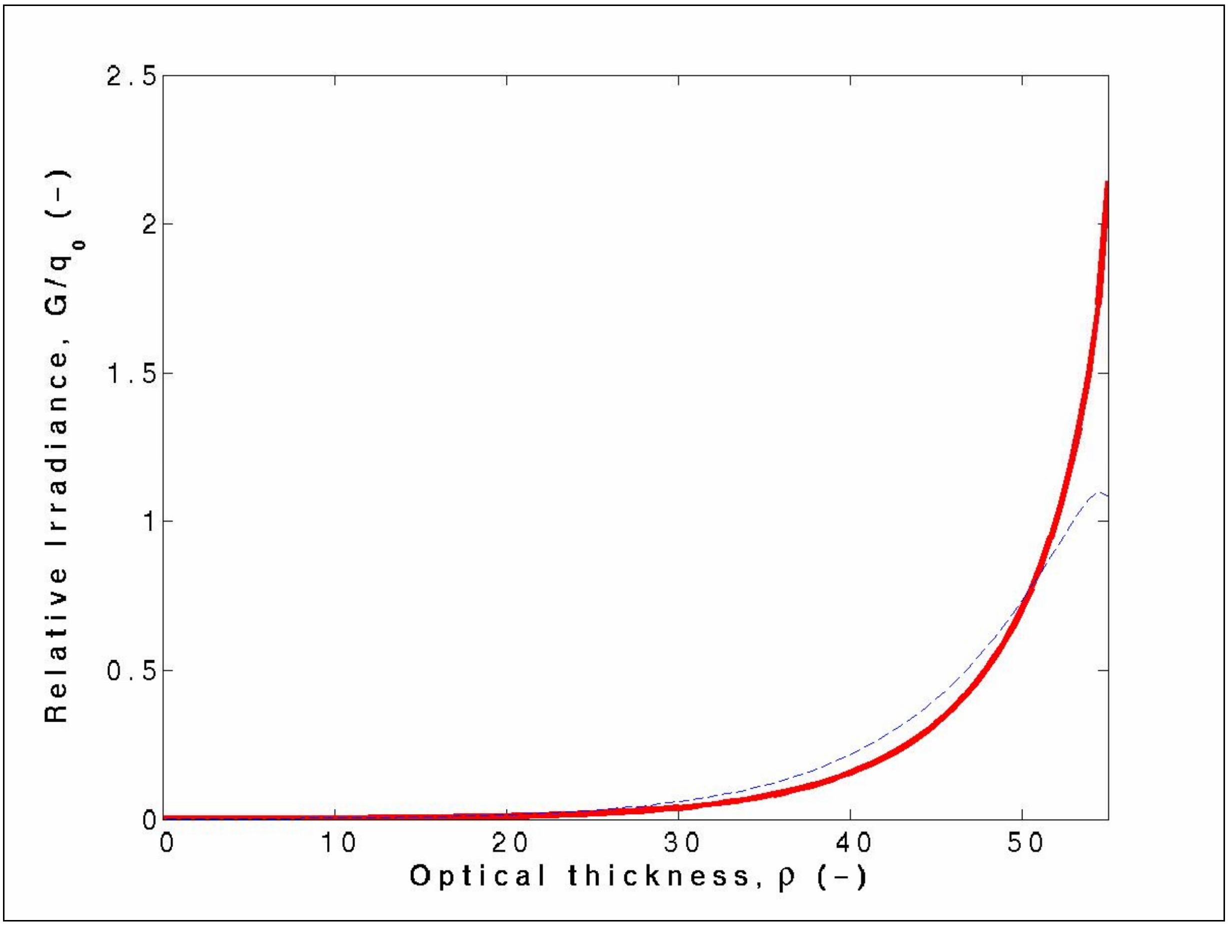

Figure A3-4 Relative light irradiance in a cylindrical system radially illuminated versus the optical thickness of the medium. Red (thick) curve corresponds to diffuse hypothesis, blue (dashed) curve corresponds to collimated hypothesis. The radiative properties of the particle used for the calculation correspond to a typical micro-organism (ω = 0.91) and are the same as in Appendix 2.

Comments on TN 83.3	Page	Answer
Equation 8: unclear in what respect the mass fraction is established (i.e. rho(dry)=kgpigment/m3organism -> what is wpig,I -> check units please)	5	wpig,i is a mass fraction (the classical pigment content) defined as kg pig / kg dry mass. As a result, k is of course a dimensionless variable. This definition has been added in the text p.5.
Please clarify: The scattering theory is built on cylindrical shaped bodies. Does this shape represent the entire organism or the photosynthetically active part of the organism?		For optical properties calculations, the shape of the micro-organism has no influence. This consideration only appears in calculating the mean real refractive index of heterogeneous particles (like bacteria) as briefly explained in 1.1.4 p. 7, and mainly
Please clarify: Some equations seem to me to assume constant PHB content. Is this true?		The general way in calculating the optical properties from the PHB content knowledge is given by eq. 12 (p. 7). As explained at the end of paragraph 1.1.4, if the PHB content is not a constant in the process, then a new relation is required to obtain its
Please clarify: I do not understand why S3 and S4 are (always) zero for rotational axissymmetric bodies. What are the assumptions? (I never dealt with it but I was working with lasers and I don't remember S3 and S4 emtpy)	8	It is right that the simplifications in the matrix **S** would require also to examine the Mueller matrix (**F**) simplifications that we have omitted to discuss here in order to simplify the presentation. Actually, the result $S_3 = S_4 = 0$ comes from the assumptio
Equation 28: no Gamma function to disting	11	The absorption and scattering coefficients are intrinsic properties of particles, independent of the field of radiation. The correction factor distinguishing between collimated and diffuse field of radiation appears only in the mathematical treatment of t
Please clarify: with an aspect ratio of 5 the neglection of the end surfaces in the scattering theory is valid?	15	Both T-matrix and Anomalous Diffraction approximation are able to deal with the exact shape of the particle (i.e. a prolate cylinder for *Rs. rubrum* and *A. platensis*). With asphericity ratio higher than 4 or 5, which is the case of these two microorganisms
Please clarify: It is stated that the refractive index is >>1; does this mean that the membrane is non-participating and no transfer losses?	15	Here again, the particle is optically considered as a whole. The Anomalous Diffraction approximation just states that **if the relative refractive index is close to 1 (and for sufficiently high size parameters *x*)**, the reflection becomes negligible in the sc
Plase clarify: If we make 'averaging assumptions'; how big is the impact?		page ? don't find in the text
Perhaps it is a good idea to state where we started (I.e. equations 63 and table above)	28	Done in the text

Suggestion: I believe there could be added value in a discussion what model to use when: I have not much experience in this field and would propose to distinguish between the models to use for academic purposes (knowledge models) and models suitable for e		This is of course a crucial point which will be discussed extensively in the following TN 83.3 from the comments of experimental results. A special attention will be paid in the comparison between experimental results and the different assumptions. Conclu
I agree, let's stay one-dimensional in radial coordiantes as the end sections are probably negligible VS. the cylindrical section of a long reactor.		
Do not understand last paragrapgh of section 4. Why is the error never more than 10%? Please explain.	42	In case of physical limitation by light, the mean VREA <A> may be obtained by averaging the LVREA on the material phase of the PBR, or directly from the radiant energy balance on the photonic phase of the PBR (knowing q_0, the specific illuminated area, an
Please use MELiSSA TN template		Done
I am curious of the dimensions of Rhodo VS wavelengths of interest. Could you just mention it in the TN?		The characteristic sizes for *Rs. rubrum* is roughly 1μm diameter and 4-5 μm long; the same dimensions for *A. platensis* are respectively 8 and 300 μm. These characteristics, together with the distribution laws and equivalent volume diameters will be discuss